OpenWQ v.1: A multi-chemistry modeling framework to enable flexible, transparent, interoperable, and reproducible water quality simulations in existing hydro-models

Diogo Costa[1], Kyle Klenk[2], Wouter Knoben[2], Andrew Ireson[2], Raymond J. Spiteri[2], and Martyn Clark[3]

[1]Mediterranean Institute for Agriculture, Environment and Development & Global Change and Sustainability Institute, Department of Geosciences, Universidade de Évora, Pólo da Mitra, Ap. 94, 7006-554 Évora, Portugal
[2]University of Saskatchewan, 110 Administration Pl, Saskatoon, SK S7N 5A2, Canada
[3]University of Calgary, 2500 University Drive NW, Calgary Alberta T2N 1N4, Canada

Correspondence: Diogo Costa (diogo.costa@uevora.pt)

Abstract.

This work advances the cross-model deployment of ecological and biogeochemical simulation capabilities in existing process-based hydro-modeling tools, which we term "Open Water Quality" (OpenWQ). We detail aspects of OpenWQ's architecture that enable its plug-in type incorporation into existing models, along with its innovative aspects that enable biogeo-chemistry lab-like capabilities. OpenWQ's innovative aspects allow modelers to define the pollution problem(s) of interest, the appropriate complexity of the biogeochemistry routines, test different modeling hypotheses, and deploy them across different hydro-models. A coupling recipe for linking OpenWQ to existing hydro-models is described and demonstrated on two models with different model structures, SUMMA and CRHM. Such model integration helps establish a more formal (and direct) exchange of innovation between hydrological and biogeochemical-water quality modeling communities. Example applications of different pollution studies enabled by OpenWQ are provided with robust numerical verification.

1 Introduction

There are considerable challenges in defining the appropriate complexity, scale, and scope of water quality models (Costa et al., 2020a; Moore et al., 2006; Mekonnen, 2016; Shoemaker, 1997). These challenges are in part due to uncertainties associated with the prediction of many hydrological and biogeochemical responses at different spatial scales and geographical settings, which are aggravated by the often sparse water quality data available for testing and validation of models. This raises critical questions for the design, application, and benefit of such modeling tools (Beck, 1987; Moore et al., 2006; Wade et al., 2008; Costa et al., 2020a). Improving process-based hydro-biogeochemical models for terrestrial hydrological simulations requires effective and continuous integration and interoperation of models across several research areas, including hydrology, biogeo-chemistry, and soil science. Models must combine practical aspects related to model application with theoretical scientific insights at various degrees of scientific maturity and geographical applications. Such cross-disciplinary modeling efforts require modelers to make model development decisions based on considerations that include (1) model fidelity, complexity and practicality, (2) scientific reproducibility and transparency, and (3) data availability (Clark et al., 2011). More flexible water

quality modeling approaches have been recognized as a pathway to help address these issues (Yang et al., 2022; Costa et al., 2020c, 2016). Some approaches have emerged that address some of the challenges and improve transparency and engagement among hydrologists, biogeochemists, soil scientists, and decision-makers, such as the STELLA (Structural Thinking and Experiential Learning Laboratory with Animation) software (Richmond, 2004) and the MIKE Eco Lab, which is a water quality modeling addition to the MIKE tools (Refsgaard and Storm, 1995). However, such tools are not suitable for integration into modeling platforms developed by the various hydrological communities around the world. In the case of STELLA, the tool is standalone and more suitable for applications where simpler batch-reactor assumptions are applicable, such as for small reservoirs and wastewater treatment plants. The MIKE tools from DHI now provide an Eco-Lab module for more flexible water quality and ecological simulations, but this module is a proprietary tool integrated within the MIKE ecosystem of tools, so it does not benefit the wider hydrology and modeling communities, and it is constrained by the chemical constituents and types of biogeochemical processes that are explicitly introduced by the MIKE model developers. More recently, Yang et al. (2022) proposed a new model named HiWaQ for flexible catchment water quality assessments with compatibility for multiple hydrological model structures. This is a valuable contribution toward a more unified and interoperable hydrological-water quality modeling approach, but the current version is limited to hydrological models and the nitrogen cycle.

The purpose of this paper is to summarize the development of a flexible multi-chemistry modeling framework (OpenWQ) that provides portable and interoperable water quality simulation capabilities for existing hydro-models. OpenWQ is a tool that (1) can be plugged into existing process-based hydrological, hydrodynamic, and groundwater models to extend their capabilities to environmental and ecological studies, (2) offers a flexible platform for tailoring chemical-microbiological constituents and biogeochemistry-cycling processes to allow the representation of different pollution problems and landscapes, and (3) enables the systematic and controlled testing of modeling hypotheses.

The goals of this paper are three-fold:

1. Describe the OpenWQ concept and how it contributes to increasing transparency, interoperability, reproducibility, and flexibility in hydro-biogeochemical studies of aquatic ecosystems.

2. Demonstrate how OpenWQ can be integrated into existing hydro-models (illustrated by two examples, SUMMA and CRHM)

3. Demonstrate how models coupled to OpenWQ can be used to examine a variety of pollution problems (with several examples and numerical validation).

The remainder of this paper is organized as follows. In Section 2 we review existing water quality models, in Section 3 we introduce the OpenWQ concept, in Section 4 we describe applications of OpenWQ demonstrating coupling procedure and testing pollution scenarios, in Section 5 we present results for a set of synthetic test cases, in Section 6 we present a discussion of the results, and in Section 7 we summarize the major contributions of this paper.

2 Existing water quality models

55 Widely used process-based catchment water quality models such as SWAT, HYPE, and INCA have been at the forefront of innovation, paving the way for researchers and decision-makers around the world to investigate solutions to a variety of pollution problems, particularly related to nutrient pollution. These models have become increasingly complex and heavily parameterized, but like most hydrological and water quality models they remain a limited representation of reality because hydro-biogeochemical processes are highly complex in natural environments (Wade et al., 2008; Beck, 1987; Costa et al.,
60 2020b). These models typically simulate a series of biogeochemical processes conceptualized to address particular pollution problems, and processes are represented through a combination of empirical and physicochemically based methods, often leading to several calibration parameters and thus increasing the risk of parameter equifinality (Costa et al., 2020b). Sparse and sporadic water quality measurements, which are common problems for most water bodies, limit the further application and development of these water quality models.

65 The combination of process-representation methods with varying degrees of empiricism is in part due to knowledge gaps in understanding the drivers and controls of hydrological and biogeochemical responses at various spatial scales and across different landscapes and climate zones. In regions where relatively uncommon processes may play an important role in the overall water quality dynamics, the use of these models becomes problematic because there is little flexibility for adjusting conceptual models, adding or removing processes, or testing different modeling hypotheses. For example, research has shown
70 that in some cold regions, processes such as preferential infiltration of hydrochemical into frozen soils (Lilbaek and Pomeroy, 2007), preferential elution of hydrochemicals from melting snowpacks (Davies et al., 1987; Marsh and Pomeroy, 1999; Costa and Pomeroy, 2019), microbial uptake and fixing of nitrogen in melting snowpack (Jones, 1999), volatilization of nitrogen during snow redistribution and sublimation (Pomeroy et al., 1991, 1999), and snowmelt nutrient release from snow–plant residue mixtures (Costa et al., 2019) may affect water quality, but they are not represented in most popular models. This lack
75 of representation may compromise the use of these existing models in such regions and calls for a more flexible, reproducible, transparent, and interoperable approach to water quality modeling that enables a systematic and controlled approach for the addition, removal, and adjustment of processes as needed to reflect (1) regional and climate characteristics, (2) data limitations, and (3) objectives of the study.

3 The OpenWQ concept

80 OpenWQ aims to address three major challenges with existing water quality models: (1) structural rigidity in the representation of chemical constituents and biogeochemical processes, (2) limitation of background hydro-flux calculations, and (3) inadequacy for testing different modeling hypotheses for proper quantification of structural uncertainty. Structural rigidity is the limitation that perhaps hinders more the effective use of models across landscapes and in complex, diverse environments (e.g., permafrost, peatlands, variable contributing areas) that require more investigative, open-ended, and interactive simulation
85 approaches.

3.1 General architecture

OpenWQ separates the physics and biochemistry calculations from the numerical implementation. Such an approach was implemented in the SUMMA model (Clark et al., 2015a, b), and we adopted it here to improve scalability and interoperability. This approach addresses a major problem with many hydrological, hydrodynamic, and water quality models where the spec-
90 ification of the model equations is intertwined with their numerical solution (Clark and Kavetski, 2010). This specification complicates the selection and assessment of different model representations (hypotheses) and makes introducing and evaluating alternative numerical methods challenging. As such, state variables in OpenWQ are only updated inside its numerical solver based on rates of mass change (time and space derivatives) computed by the different physical and biogeochemical process routines. The current numerical solution is based on the simple finite-volume forward Euler method because at this stage pri-
95 ority has been given to developing the overall model concept, architecture, and testing capabilities (proof of concept). Yet, the fundamental separation of the numerical solver from the physics-biogeochemistry calculations enables the future improvement of the numerical implementation in a controlled manner.

There are four core space-time derivatives altering the state-variables in OpenWQ that relate to (1) initial conditions (dm_ic), (2) sinks and sources of chemical load (i.e., chemical mass entering or exiting the model domain) (dm_ss), (3) biogeochemical
100 processes ($dm\_dt\_chemistry$), and (4) physical transport of chemical constituents with water flow ($dm\_dt\_transport$). This is depicted in Fig. 1. However, different modules (blue boxes) and model options (outer beige boxes) can be activated or deactivated for the calculation of each of these derivatives. The number of modules and model options available will grow with future developments.

OpenWQ adapts to the hydro-model spatial and temporal discretization structure, which can include Hydrological Response
105 Units (HRUs), 1D–3D spatial distributed meshes, structured or unstructured meshes, and multiple domains or hydrological compartments (e.g., snow, soil, groundwater). OpenWQ's state variables (column 1 in Fig. 2) are stored in a hierarchical data structure organized with the following nested fields: (1) domain that refers to hydrological compartments (column 2 in Fig. 2), (2) chemical species (column 3 in Fig. 2), and (3) sub-domain that refers to the internal 1D–3D spatial discretization of the domains or hydrological compartments (column 4 in Fig. 2). The hierarchical data structures are built via the Armadillo
110 C++ library for linear algebra and scientific computing (Sanderson and Curtin, 2016, 2018). The state-variable data structures record the spatiotemporal evolution of the mass of the different chemical species tracked in each model domain or hydrological compartment (e.g., snow, soil, groundwater).

3.2 Portability and interoperability via dynamic coupler

In order to optimize the integration of OpenWQ into existing hydro-models, the model has been designed as an internal
115 coupler module. External coupling (i.e., OpenWQ reading output files from the host-model and running standalone) was not a viable option because hydro-models, particularly hydrological models, typically deal with multiple water fluxes moving around vertically and horizontally within and across hydrological compartments (e.g., snow, soil), which are not always exportable nor possible to disentangle. Even in cases where models allow exporting all water fluxes separately, externally re-mapping those in
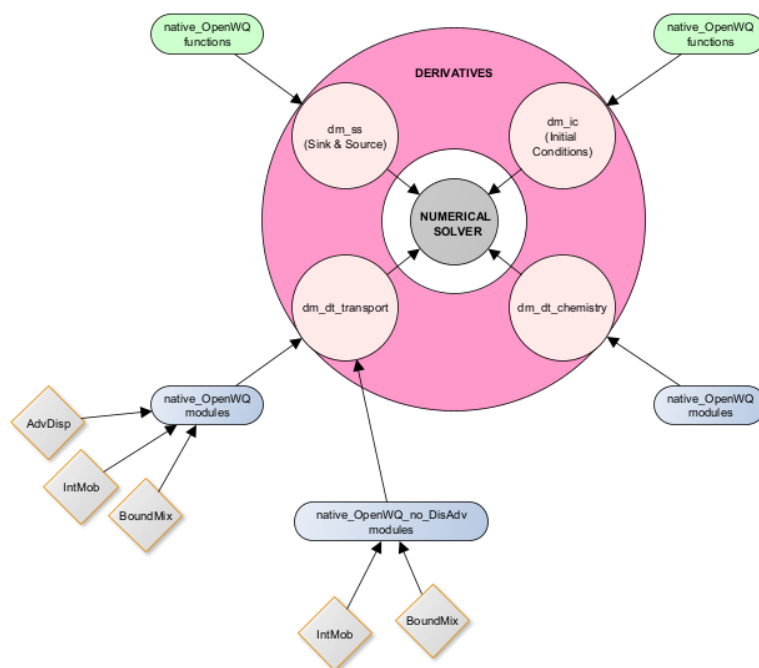
Figure 1. General modular architecture of OpenWQ computes four core space-time derivatives (light-pink circles) via a series of modules (blue and green boxes) and module options (outer beige boxes).

OpenWQ while harmonizing units to correctly compute the corresponding solute mass transport would be extremely difficult
120 for most applications and prone to problems. Focusing on a flexible full-coupling strategy with minimal code re-engineering allowed us to address this problem and guarantee adequate communication between OpenWQ and the (host) hydro-models. Although interface and coupler functions may need adjustments to harmonize particular specificities of each hydro-model, a generic "hydro-link" file has been developed with a template for these functions. It is possible to create such a template because most hydro-models follow the general model architecture depicted in Fig. 3 (grey boxes).

125   The integration of OpenWQ into existing hydro-models is carried out through four coupler functions (pink boxes, Fig. 3) that are responsible for (1) converting datatypes and data structures between OpenWQ and the "host" hydro-model, (2) passing hydro-fluxes into OpenWQ, and (3) calling OpenWQ's APIs. This is a one-way communication from the host hydro-model to OpenWQ, so no information is returned to the host model. The interface functions are generic and serve as templates (coupling recipes) that have been optimized to streamline the coupling procedure. The adjustments needed in the interface functions are
130 to ensure that the data types and structure used in the hydro-model are properly translated into OpenWQ's own data structure and conventions so that OpenWQ's APIs can perform adequately.
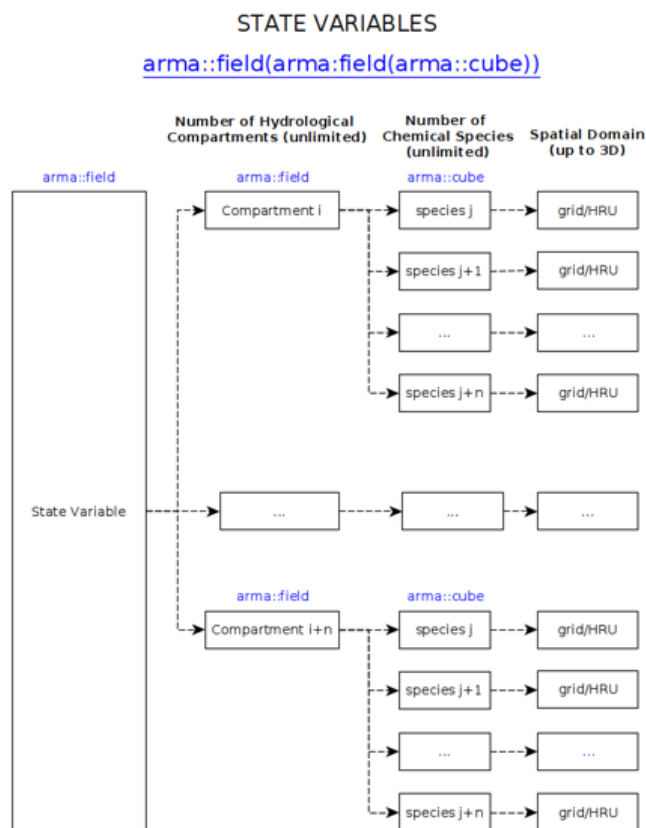
Figure 2. State variables are stored in OpenWQ via dynamic hierarchical data structures

3.3 Current modules and options

OpenWQ contains modules to deal with (1) initial conditions, (2) sinks and sources, (3) transport (advection and dispersion) with water, and (4) biogeochemistry (see Fig. 1). The first two groups of modules deal with initial conditions and sinks and external sources with a focus on translating user inputs into the simulation. For example, the sink and source module applies chemical load as prescribed by the users that can include (1) continuous load arising from sources like atmospheric deposition or the outlet of a wastewater treatment plant or (2) episodic/instantaneous loads arising from sources such as fertilizer and chemical spills. The remaining two groups of modules focus respectively on (1) the physical transport of chemical constituents as water moves through the system and (2) biogeochemical transformations.

3.3.1 Transport Module

Currently, there are two options available for computing the physical transport of dissolved solutes and fully suspended sediments. The first option accounts for both advection and dispersion and solves the hyperbolic-parabolic advection-diffusion
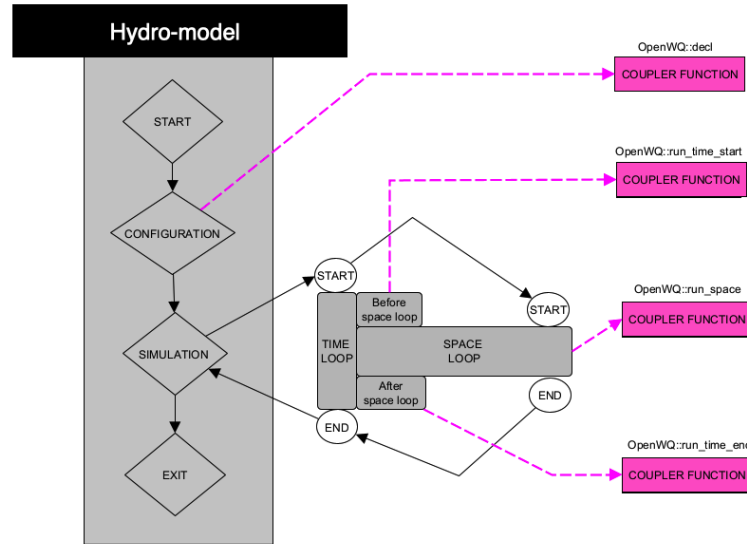
Figure 3. General mechanistic hydro-model structure (grey boxes) and where OpenWQ's four coupler functions are called (pink boxes)

partial differential equation (PDE) in up to 3 dimensions depending on the host model spatial discretization scheme (Equation 1); the second option only accounts for advection (Equation 2). In both cases, the PDEs are solved inside OpenWQ's numerical

145 solver as described in Section 3.1 using the hydro-model fluxes. This means that for each water flux computed by the host-model (at each grid cell and timestep), OpenWQ calculates the corresponding solute mass transported. The physical transport can be between computation elements (e.g., HRUs, grid cells) and across domains or hydrological compartments (e.g., runoff, soil saturated, soil unsaturated, canopy), as prescribed by the host hydro-model. New modules and model options can be easily added.

$$\frac{\partial (Vc_s)}{\partial t} + \nabla \cdot (V\boldsymbol{u}c_s) = \nabla \cdot (V\mathbf{E} \cdot \nabla c_s) + S, \tag{1}$$

$$\frac{\partial (Vc_s)}{\partial t} + \nabla \cdot (V\boldsymbol{v}c_s) = S, \tag{2}$$

where V is the volume of the computational element/cell [L^3]; c_s is the concentration of a given dissolved substance [ML^{-3}]; $\boldsymbol{u} = (u_x, u_y, u_z)$ is the velocity in the x, y, and z directions [LT^{-1}]; $\mathbf{E}$ is the (diagonal) diffusivity tensor [L^{2}T^{-1}]; and S is a source term [MT^{-1}] that is linked to the chemistry modules. The $\mathbf{E}$ term accounts for the combined effect of different mixing

155 phenomena. L, M and T are the dimensions of Length, Mass and Time, respectively. This notation is used throughout the manuscript.

3.3.2 Biogeochemistry module

Biogeochemical cycling and transformations are customizable via JavaScript Object Notation (JSON) files. Each cycling framework is given a "tag" that is used for loading into simulations through OpenWQ's main configuration file. The char-

acterization of each of these cycling frameworks involves the definition of biogeochemical transformations and the chemical species involved. In turn, the characterization of each of these transformations requires information about the chemical species consumed and produced and the reaction kinetics. OpenWQ's kinetics solver is based on the C++ Mathematical Expression Toolkit Library (*ExprTk*) developed by Arash Partow (1999–2020) (Partow, 1999). The implementation of *ExprTk* in OpenWQ is simple to use and provides an efficient run-time mathematical expression parser and evaluation engine. It supports numerous forms of functional, logical, and vector processing semantics and is easily extendable. The equations can be written with (1) multiple chemical species, (2) user-defined parameters, and (3) built-in hydro-model variable dependencies.

The biogeochemistry JSON input file can be prepared manually following the appropriate OpenWQ JSON structure (i.e., key-value pairs). Alternatively, the cycling frameworks can be created via a diagram drawn using a *GraphML* editor, which can then be converted into OpenWQ's JSON format using a Python script (named "Convert_graphml_BGCjson.py") available in OpenWQ's public repository. This graphical option aims to foster collaboration between modellers and (water and soil) biogeochemists. Although the expressions used to represent the different reaction kinetics in the model (via the biogeochemistry JSON files) can take many forms, sequences of reaction networks are often used involving single or multiple chemical species governed by zero-, first-, second-, or third-order kinetics as described in Eqs. 3 to 6, respectively.

$$\frac{dc_A}{dt} = -k\lambda, \tag{3}$$

$$\frac{dc_A}{dt} = -k\lambda c_A, \tag{4}$$

$$\frac{dc_A}{dt} = -k\lambda c_A^2, \tag{5}$$

$$\frac{dc_A}{dt} = -k\lambda c_A^2 c_B, \tag{6}$$

where c_A and c_B [ML^{-3}] are the concentrations of chemical species A and B, parameter/variable λ represents weather/hydrological dependencies (such as soil moisture and temperature) [-], and k is the reaction rate constant where the units vary depending on the reaction order: ML^{-3}T^{-1}, T^{-1}, M^{-1}L^{3}T^{-1}, and M^{-2}L^{6}T^{-1} for respectively zero-, first-, second and third order reactions. The reaction rate k can be provided as the reaction rate using standard maximum at a reference temperature (often 20°C) or using expressions that can include relationships with the hydrological/weather-dependent variables/parameters.

3.4 Inputs and Outputs

The configuration of OpenWQ is provided via four JSON files. Each of these files deals with a particular aspect of the model setup and is given one of the following designations (1) "runManagement" (general simulation instructions), (2) "Biogeochemistry" (characterization of biogeochemical cycles, as described above), (3) "Configuration" (initial conditions and loading the desired biogeochemical cycles and options to simulate) and (4) "Source/Sink" (input or output of chemicals, e.g., fertilizer input). Simulation instructions and options in these JSON files are provided via key/value pairs, e.g., "RUN_MODE_DEBUG: TRUE".

4 Application of OpenWQ: Demonstrating coupling procedure and testing pollution scenarios

4.1 Coupling to two existing hydro-models

The OpenWQ concept has been demonstrated through coupling to two hydro-models, SUMMA (Clark et al., 2015a, b) and CRHM/CRHM-WQ (Pomeroy et al., 2022; Costa et al., 2021; Pomeroy et al., 2007). SUMMA is written in Fortran, while OpenWQ is written in C++. Thus, it was necessary to create wrapper functions that allow for the interaction between a Fortran driver program (SUMMA) and a C++ coupled program (OpenWQ) at runtime. This coupling was performed using the standard Fortran module *iso_c_binding* that defines constants, types, and procedures for C interoperability. Fortran-to-C wrapper functions were created to allow SUMMA to interface with OpenWQ and, from the point of view of SUMMA, OpenWQ is an object to which a pointer is held upon initialization of OpenWQ. The wrapper functions allowed SUMMA to interface with OpenWQ's coupler functions as if they were method calls. Fortran-to-C wrapper functions were constructed for creating a reference to OpenWQ along with each of the four OpenWQ C++ coupler functions (*openwq::decl*, *openwq::run_time_start*, *openwq::run_space*, and *openwq::run_time_end* - see Fig. 3). In turn, CRHM is written in C++, the same programming language of OpenWQ. Accordingly, the need for wrapper interface functions was avoided. Yet, in this case, CRHM already had a water quality module named CRHM-WQ that enables the specific simulation of the nitrogen (N) and phosphorous (P) cycles (Costa et al., 2021). Thus, CHRM already contained a solute transport simulation routine that moves contaminants through the hydrological cycle represented by the model. Therefore, instead of coupling all four OpenWQ coupler functions to CRHM-WQ, we considered it more appropriate to use CRHM's native transport routine, which had already been tested by (Costa et al., 2021), leaving OpenWQ's coupling routine for transport (*openwq::run_space*) out of the coupling process and, this way, demonstrating the flexibility of OpenWQ's model structure and coupling procedure.

4.2 Test cases

In recent years, it has been recognized that basic tests to evaluate the robustness of model mathematical formulations and numerical solutions are essential for proper model scrutiny, falsification, and acceptance (Clark et al., 2021a). In this study, we extended these principles to water quality simulations where the spatiotemporal complexity and interplay of process generally often give rise to highly non-linear response patterns that are difficult to disentangle in real-world applications for proper model examination (Costa et al., 2022, 2020a). We prepared a total of ten tests, of which two are non-reactive (biogeochemistry deactivated), and eight are reactive (biogeochemistry activated) - see Table 1. The test cases are representative of a variety of environmental pollution problems for which analytical solutions have been either specially derived for this paper or taken from the literature (see Appendix A). The test cases include six batch reactor-type tests, specifically two single-species tests and four multi-species tests. The single-species tests are the simplest and represent cases involving first- (Test 1) and second-order (Test 2) linear decay processes. The multi-species tests include (a) a two-species reaction network subject to linear decay (Test 3), (b) a three-species reaction network subject to linear decay (Test 4), and reaction networks to represent the (c) nitrogen (Test 5) and (d) dissolved oxygen (Test 6) cycles. The remaining four tests involve the transport of chemical constituents, specifically two non-reactive tests, one considering a continuous point source (Test 7), one considering an instantaneous points

Table 1. Model configuration for the different test cases

Transport Scheme	Designation	Reference	Biogeochemistry		
			Initial Conditions	Reaction kinetics	Transport
Batch Reactor	1_noTrans_1species_1storder	Fig. A1	Species A (c_0 = 10 mg/l)	$k_{transf\_A} = 0.01\ 1/day$	NA
	2_noTrans_1species_2ndorder	Fig. A1	Species A (c_0 = 10 mg/l)	$k_{transf_A} = 0.01 1/day$	NA
	3_noTrans_2species	Fig. A2	Species A (c_0 = 10 mg/l)	$k_{transf\_A} = 0.03\ 1/day$	NA
			Species B (c_0 = 0 mg/l)	$k_{transf\_B} = 0.01\ 1/day$	
	4_noTrans_3species	Fig. A3	Species A (c_0 = 10 mg/l)	$k_{transf\_A} = 0.03\ 1/day$	NA
			Species B (c_0 = 0 mg/l)	$k_{transf\_B} = 0.01\ 1/day$	
			Species C (c_0 = 0 mg/l)	$k_{transf\_C} = 0.005\ 1/day$	
	5_noTrans_nitrogencycle	Fig. A4	Nref (c_0 = 10 mg/l)	$k_{degrd} = 0.006\ 1/day$	NA
			Nlab (c_0 = 10 mg/l)	$k_{dissol-1} = 0.0002\ 1/day$	
			DIN (c_0 = 5 mg/l)	$k_{dissol-2} = 0.0003\ 1/day$	
			DON (c_0 = 2 mg/l)	$k_{miner} = 0.003\ 1/day$	
				$k_{denitr} = 0.001\ 1/day$	
				$k_{plantup} = 0.001\ 1/day$	
	6_noTrans_oxygenBODcycle	Fig. A5	BOD (c_0 = 10 mg/l)	$k_{BODdegrad} = 0.1\ 1/day$	NA
			DO (c_0 = 12 mg/l)	$k_{reaertion} = 0.5\ 1/day$	
Advection-Dispersion	7_trans_contS_PorMedia	NA	Species A (c_0 = 0 mg/l)	NA	$D_z = 0.0001\ m^2/s$
	8_trans_contS_PorMedia_1storder	Fig. A1	Species A (c_0 = 0 mg/l)	$k_{transf\_A} = 0.01\ 1/day$	$D_z = 0.0001\ m^2/s$
	9_trans_instS_PorMedia	NA	Species A (c_0 = 0 mg/l)	NA	$D_z = 0.0001\ m^2/s$
	10_trans_instS_PorMedia_1storder	Fig. A1	Species A (c_0 = 0 mg/l)	$k_{transf\_A} = 0.01\ 1/day$	$D_z = 0.0001\ m^2/s$

source (Test 8), and two reactive tests that are similar to the homologous non-reactive tests, but where chemical species undergo biogeochemical transformations (Tests 9 and 10, respectively). In the case of Tests 7 to 10 (transport simulations), testing was

225   only meaningful for SUMMA-OpenWQ because, as previously mentioned, the coupling of OpenWQ to CRHM-WQ did not contemplate OpenWQ's transport routines because CRHM-WQ contains its own transport module. For SUMMA-OpenWQ, Tests 7 to 10 were based on the soil unsaturated flow test cases formulated by Celia et al. (1990), which have been set up as described in Clark et al. (2021b). The soil properties of these tests are described in Table 2 of that paper.

The model results have been compared to the respective analytical solutions to verify the accuracy of OpenWQ in examining

230   a variety of pollution problems. These tests contemplate several biogeochemical processes that are often the object of study in environmental studies. The Nash-Sutcliffe efficiency coefficient (NSE, Eq. 7) and the Root-Mean-Square Error (RMSE, Eq. 8) were used to quantify the accuracy of the numerical results.

$$\text{NSE} = 1 - \frac{\sum(X_{obs} - X_{mod})^2}{\sum(X_{obs} - \mu_{obs})^2}, \tag{7}$$

$$\text{RMSE} = \sqrt{\frac{\sum(X_{obs} - X_{mod})^2}{n}}, \tag{8}$$

where X_{obs} and X_{mod} are the observed and simulated concentrations, μ_{obs} is the concentration average, and n is the number of observations. NSE values equal to one indicate a perfect match between observations and model results, and NSE values equal to zero indicate model predictions as accurate as the mean of all observations.

5 Results

5.1 Batch reactor: Single-species (Tests 1 and 2)

The results of Tests 1 and 2 contemplate the general cases of single chemical species subject to first- or second-order decay as presented in Fig. 4. Such reaction types are commonly used in sequence or parallel to represent complex reaction networks. The results show good model predictability and reduced numerical dispersion. For Test 1, the Nash–Sutcliffe and RMSE values obtained for SUMMA-OpenWQ were respectively 0.999999998259312 and 8.804e–05 mg/l, and for CRHM-OpenWQ were 0.999999998259309 and 8.804e–05 mg/l. For Test 2, the Nash–Sutcliffe and RMSE values obtained for SUMMA-OpenWQ were 0.999999900146240 and 3.0319e–04 mg/l, and for CRHM-OpenWQ were respectively 0.999999900145974 and 3.0319e–04 mg/l. The results obtained with SUMMA-OpenWQ and CRHM-OpenWQ are similar, which was expected because these tests deal only with biogeochemical transformations, and nutrient transport, which is driven by the host-models, is not activated. The RMSE is one order of magnitude higher for Test 2 and was also anticipated given that the biogeochemical formulation in this test contains an exponent (i.e., power of two), which magnifies the propagation of round-off errors.

(a) Test 1 (1_noTrans_1species_1storder)   (b) Test 2 (2_noTrans_1species_2ndtorder)
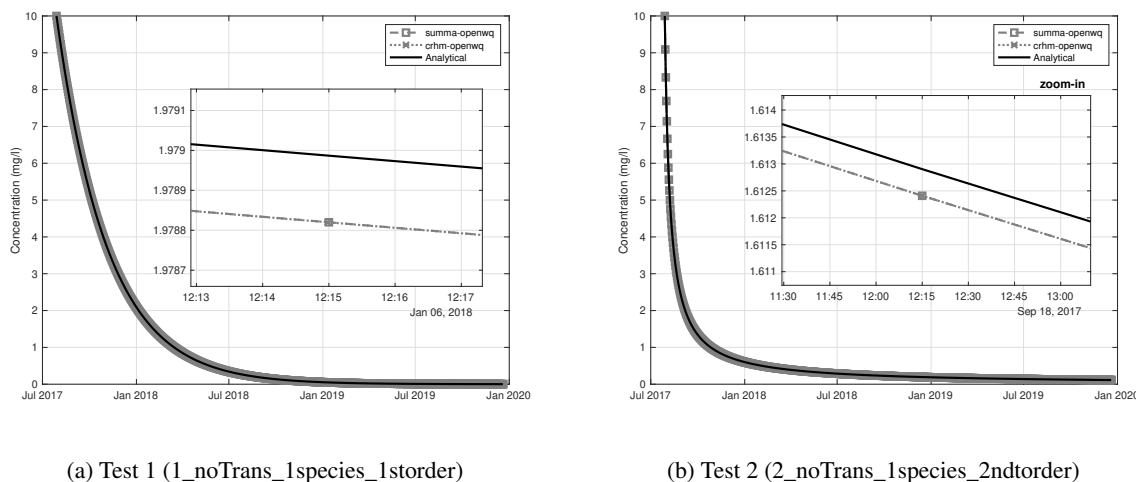
Figure 4. Comparison between model results and analytical solution for Tests 1 and 2

5.2 Batch reactor: Two-species reaction network (Test 3)

The results of Test 3 are presented in Fig. 5 and compared against analytical solutions. Two-species reaction networks are also common in water quality models and often integrated within comprehensive biogeochemical cycling representations. The model shows good agreement with the analytical solution for Test 3, including the results for both Species A and B. For Species A, the Nash–Sutcliffe and RMSE values obtained for SUMMA-OpenWQ were 0.999999987172389 and 1.525e–04 mg/l, and for CRHM-OpenWQ were respectively 0.999999987172368 and 1.525e–04 mg/l. For Species B, the Nash–Sutcliffe and RMSE values obtained for SUMMA-OpenWQ were 0.999999989757722 and 1.747e–04 mg/l, and for CRHM-OpenWQ

were respectively 0.999999989757706 and 1.747e–04 mg/l. The RMSE calculated for Species B is slightly higher than that calculated for Species A. This result was anticipated because the reaction network sequence starts with Species A; thus,

255 the effect of changes in the concentration of Species A will take some time to travel to Species B due to the implemented discretization. Reducing the length of the time step reduces the problem.
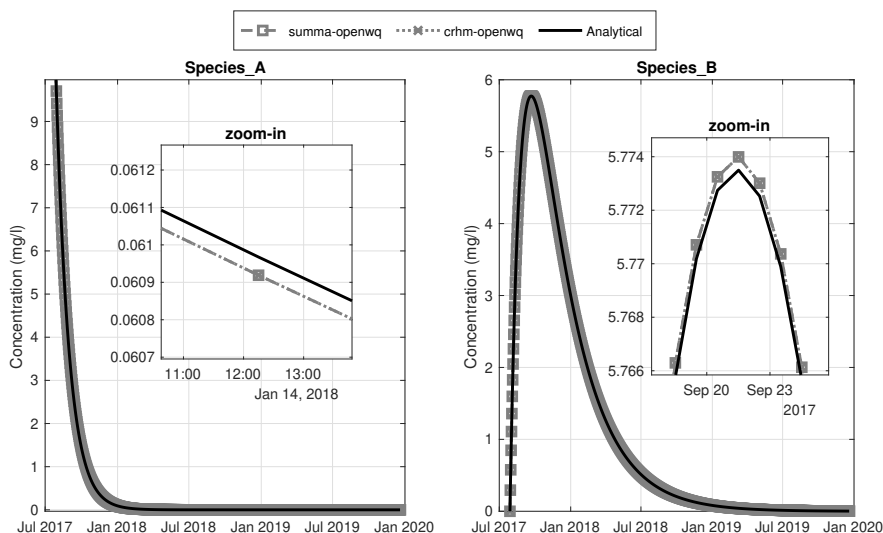
Figure 5. Comparison between model results and analytical solution for Test 3

5.3 Batch reactor: Three-species reaction network (Test 4)

Fig. 6 shows the model results for Test 4, comparing the numerical solution with the corresponding analytical solution. This constitutes a more complex reaction chain that is often integrated into more complex biogeochemical cycling frame-

260 works. Similar to the previous tests, the model demonstrates good accuracy and small numerical dispersion. For Species A, the Nash–Sutcliffe and RMSE values obtained for SUMMA-OpenWQ were respectively 0.999999987172389 and 1.524e–04 mg/l and 0.999999987172368 and 1.524e–04 mg/l for CRHM-OpenWQ. For Species B, the Nash–Sutcliffe and RMSE values obtained for SUMMA-OpenWQ were respectively 0.999999989757722 and 1.747e–04 mg/l and for CRHM-OpenWQ were 0.999999989757706 and 1.747e–04 mg/l. For Species C, the Nash–Sutcliffe and RMSE values obtained for SUMMA-

265 OpenWQ were respectively 0.999899420454185 and 1.560e–02 mg/l and for CRHM-OpenWQ were 0.999899420454600 and 1.560e–02 mg/l. A small phase shift can be noticed for Species C, which is also caused by the reaction network sequence issue mentioned in the previous test (Test 3). In OpenWQ, the hydro-models (CRHM and SUMMA) control the model time step. In these tests, the time step used was 15 minutes and was dictated by the data time intervals. The larger the time step is, the larger the shifts are expected to become because the computation of the reactions depends on the concentrations in the

270 antecedent time step. So, in this case, a change in Species A has taken 30 min (2×15 minutes) to numerically travel to Species C, producing a slight phase shift. Reducing the length of the time step reduces the problem.
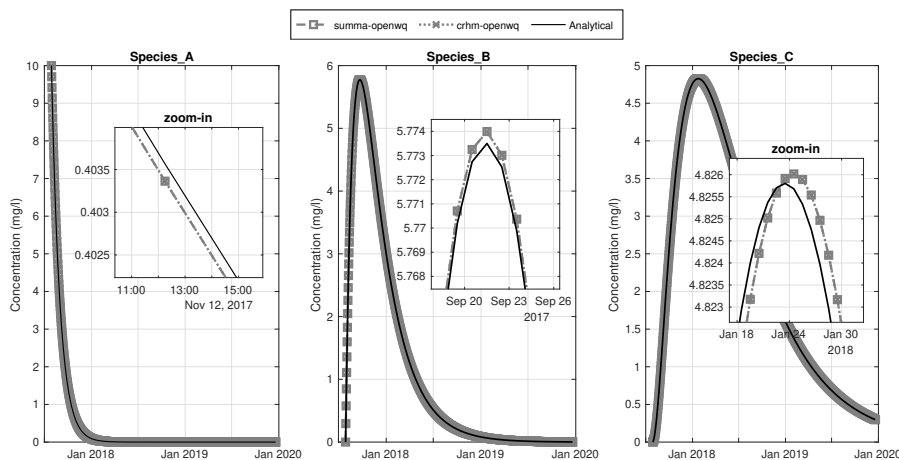
Figure 6. Comparison between model results and analytical solution for Test 4

5.4 Batch reactor: Nitrogen cycle (Test 5)

The results of the nitrogen cycle simulation show good agreement with the numerical solution (Fig. 7). This is a reaction network involving four nitrogen species, and it is commonly used in popular models such as HYPE, INCA, and SWAT. The

275 model shows good agreement with the analytical solution, reinforcing the confidence in OpenWQ's numerical solution and the implementation of the expression evaluator based on the C++ Mathematical Expression Toolkit Library (*ExprTk*) developed by Arash Partow (Partow, 1999). For Nref, the Nash–Sutcliffe and RMSE values obtained were 0.999999999184531 and 6.927e–05 mg/l and 0.999999999184529 for SUMMA-OpenWQ and 6.927e–05 mg/l for CRHM-OpenWQ. For Nlab, the Nash–Sutcliffe and RMSE values obtained for SUMMA-OpenWQ were respectively 0.999136304357914 and 9.426e–02 mg/l

280 and for CRHM-OpenWQ were 0.999136304357383 and 9.426e–02 mg/l. For DON, the Nash–Sutcliffe and RMSE values obtained were 0.999463220618209 and 1.3089e–02 mg/l for SUMMA-OpenWQ and 0.999463220618758 and 1.309e–02 mg/l for CRHM-OpenWQ. For DIN, the Nash–Sutcliffe and RMSE values obtained were 0.996669866632908 and 7.181e–02 mg/l for SUMMA-OpenWQ and 0.996669866633266 and 7.181e–02 mg/l for CRHM-OpenWQ. As in the previous reaction networks tested, the RMSE increases as the information travels through the network sequence: RMSE(DIN)> RMSE(Nref).

285 This is caused by the issue raised above related to the time of travel of information through the network sequence computation.

5.5 Batch reactor: Dissolved oxygen cycle (Test 6)

The simulation of the dissolved oxygen cycle is presented in Fig. 8 with two water quality variables (1) dissolved oxygen (DO) and (2) biological oxygen demand (BOD). This is also a common pollution problem simulated by water quality models to
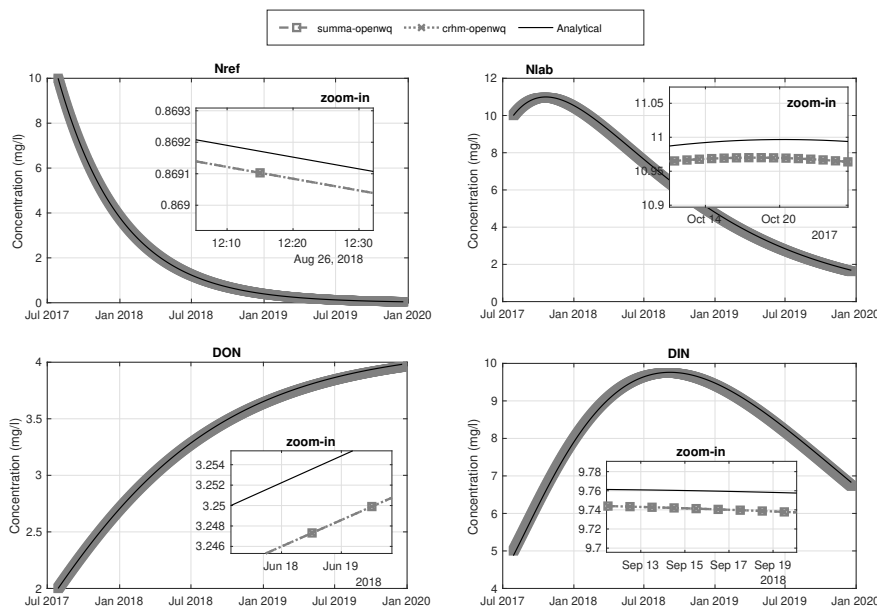
Figure 7. Comparison between model results and analytical solution for Test 5

evaluate mitigation strategies for contamination caused by urban wastewater discharges in rivers and lakes. The model shows
good agreement with observations, capturing the typical DO sag often observed near discharge outlets as predicted by the
analytical solution. For DO, the Nash–Sutcliffe and RMSE values obtained were 0.999998916342720 and 1.416e–04 mg/l
for SUMMA-OpenWQ and 0.999998916342720 and 1.416e–04 mg/l for CRHM-OpenWQ. For BOD, the Nash–Sutcliffe and
RMSE values obtained were 0.999999874118595 and 2.783e–04 mg/l for SUMMA-OpenWQ and 0.999999874118595 and
2.783e–04 mg/l for CRHM-OpenWQ. As in the previous cases, the RMSE increases through the reaction network sequence,
which is higher for BOD, despite that the Nash–Sutcliffe value remains high for both species.

5.6 Reactive and non-reactive transport: Continuous point source (Tests 7 and 8)

Fig. 9 compares model results against analytical solutions for Tests 7 and 8, which represent non-reactive and reactive scenarios
of transport of a continuous pollution source through porous media. The results show the traveling of solute through the
soil profile driven by advection and dispersion processes. In the case of Test 8 in Fig 9b, there is an additional first-order
biogeochemical reaction causing a linear decay in the concentrations. Each figure shows the computed concentrations, as well
as the model internal derivatives that have been passed into the numerical solver to compute the concentration update. This is
useful information to understand the key processes controlling the concentration of the solute as time progresses, as well as the
relative contributions of transport and biogeochemistry. Comparing Figs 9a and 9b, it becomes clear that the superposition of
the different processes (e.g., biogeochemistry, physical transport) gives rise to a highly non-linear response that the model can
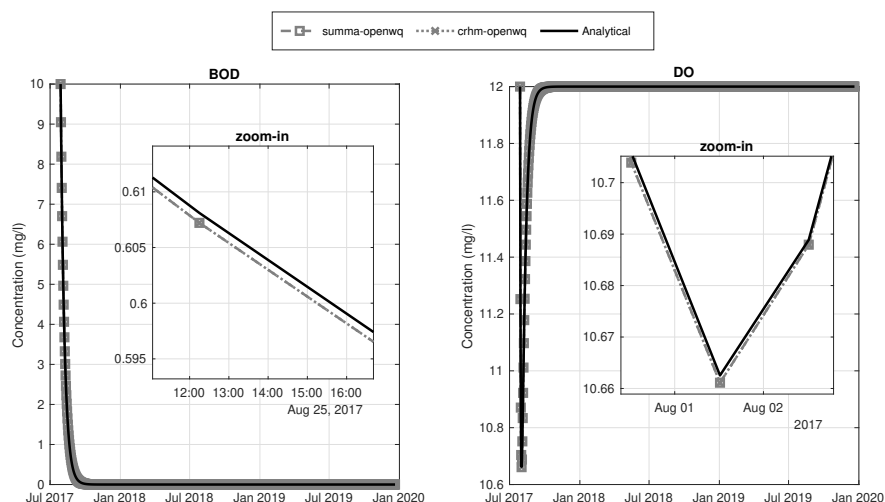
Figure 8. Comparison between model results and analytical solution for Test 6

305   capture accurately. The Nash–Sutcliffe and RMSE values obtained were 0.9890 and 0.0747e–05 mg/l for Test 7 and 0.9953 and 0.0392 mg/l for Test 8. Results show that the Nash–Sutcliffe values remain high, but they are slightly lower when compared to the purely biogeochemical kinetic Tests 1-6. The opposite is observed for RMSE, where values have slightly increased. This minor deterioration of the numerical results with the activation of the transport routines was expected, and it remains within acceptable values. This is caused by the initial conditions required to translate in the host-model to represent those set up in

310   the analytical solutions, as well as the velocity fields computed by the host model and associated numerical dispersion in both OpenWQ and the host model.

5.7   Reactive and non-reactive transport: Instantaneous point source (Tests 9 and 10)

The non-reactive and reactive tests for an instantaneous point source problem are shown in respectively Figs. 10a and 10b. Like in the previous case, there is an additional first-order biogeochemical reaction causing a linear decay in the concentrations of

315   Test 10 in Fig 10b. The Nash–Sutcliffe and RMSE values obtained were 0.9535 and 4.614e–05 mg/l for Test 9 and 0.9521 and 1.409e–05 mg/l for Test 10. The effect of biogeochemistry in the resulting concentrations can be also clearly observed in the upper-middle panel of Fig. 10a as compared to the upper-middle panel of Fig. 10b. Similar to Tests 7 and 8, results show that the Nash–Sutcliffe values remain high but are slightly lower when compared to the purely biogeochemical kinetic Tests 1–6.

6   Discussion
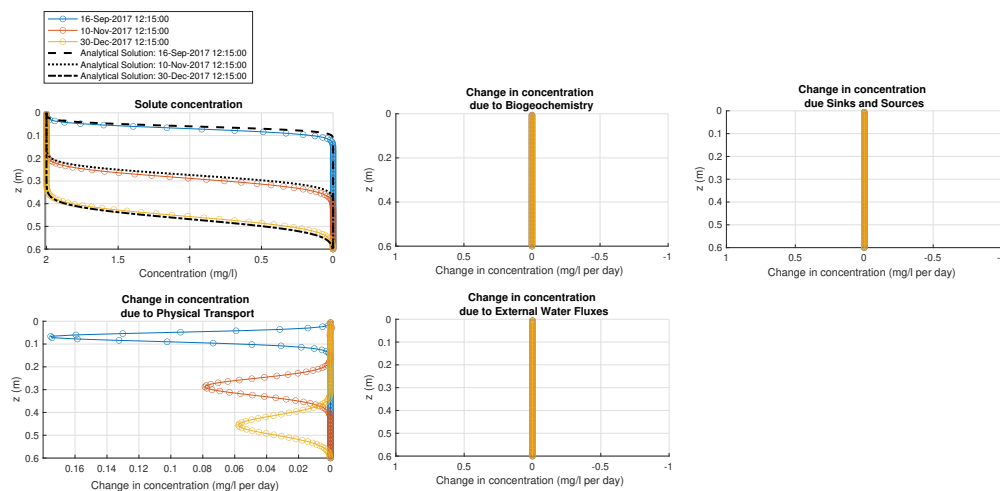
(a) Test 7
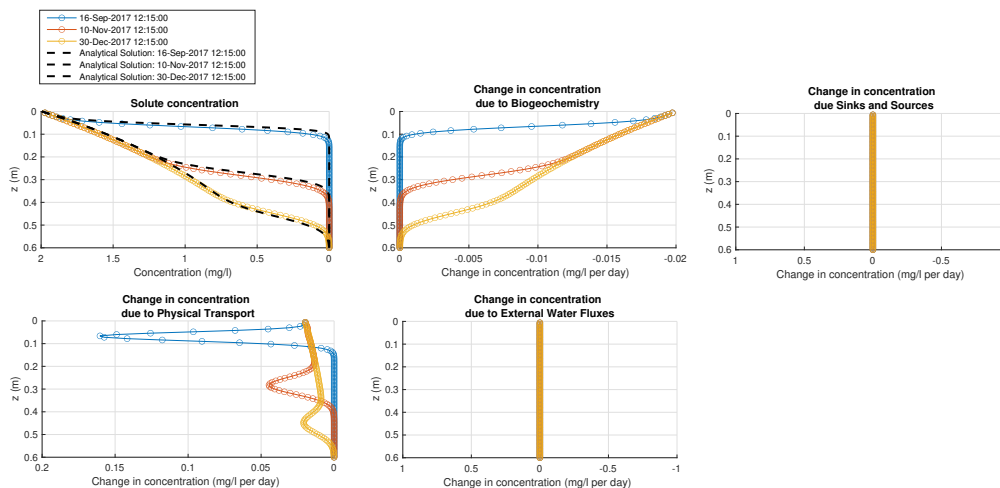
(b) Test 8

Figure 9. Comparison between model results and analytical solution for Tests 7 and 8

6.1 Interoperability, flexibility, transparency, and reproducibility - the benefits of an eco-modeling lab and cross-hydro-model deployment

320

OpenWQ's concept (as a customizable biogeochemistry modeling framework) and design (as coupled to enable cross-model deployment) is an innovation in water quality modeling that aims to promote transparent collaboration across scientific fields, including biogeochemistry, soil science, hydrology, hydrodynamics, and hydrogeology. These innovations pave the way for
325 fundamental advances in the current paradigm of water quality modeling:
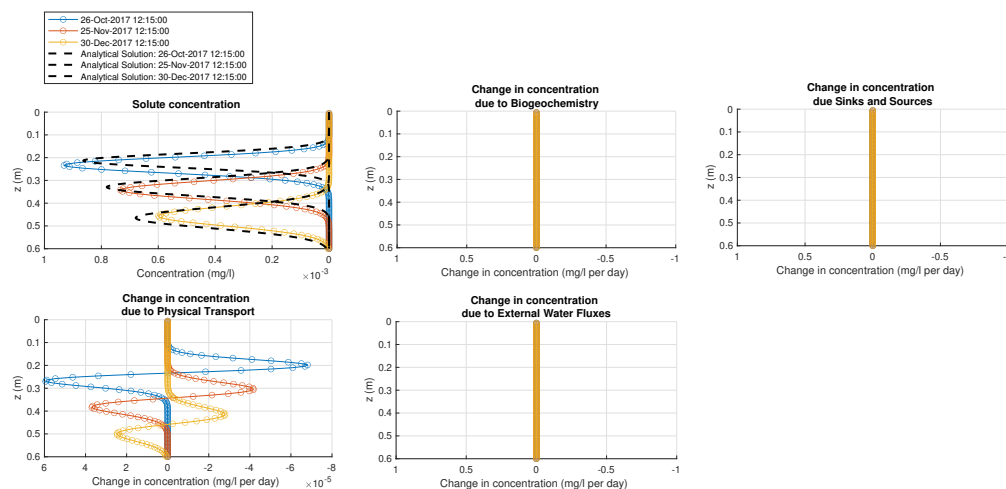
(a) Test 9
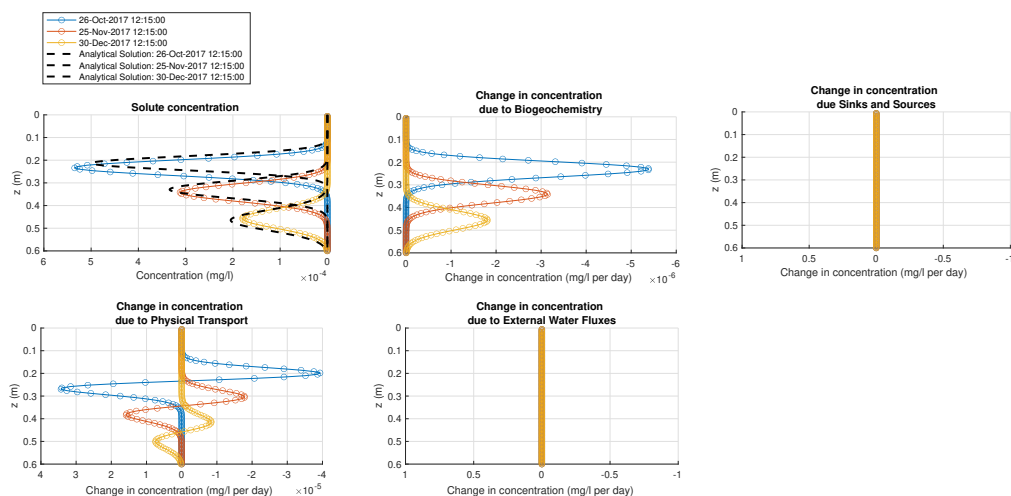
(b) Test 10

Figure 10. Comparison between model results and analytical solution for Tests 9 and 10

1. *Interoperability* (optimizing research effort): Focus given to a single biogeochemical tool that will benefit multiple hydro-models by extending their capabilities to water quality and ecological studies, thus reducing code maintenance and maximizing value;

2. *Transparency and reproducibility* (increasing confidence in simulation outputs): OpenWQ's input files can be transferred across hydro-models that have been coupled to OpenWQ, providing experience and knowledge transfer between environmental projects and research communities, as well as cross-model comparisons and replication (Fig. 11);

3. *Flexibility* (facilitating collaboration across disciplines): The ability to test different (water and soil) biogeochemical modeling hypotheses in a controlled manner allows for a more transparent and effective collaboration between modelers and hydrologists, biogeochemists, and soil scientists

6.2 Unifying multi-scale approaches to water quality modeling

OpenWQ provides a unifying modeling framework to deploy different approaches to physiochemically based soil and water quality modeling across existing hydrological, hydrodynamic, and hydrogeological models. Here, we emphasize how OpenWQ can help unify different modeling approaches to simulate different landscapes and pollution problems.

1. *Sub-catchment versus catchment-scale modeling.* OpenWQ provides a unique opportunity to harmonize spatial scales in water quality modeling. Water quality models usually belong to one of two scales regarding the spatial domain, (a) sub-catchment and (b) catchment. Sub-catchment water quality models, including river-reach models such as WASP (Wool et al., 2020; Di Toro et al., 1983) and QUAL2E (Brown and Barnwell, 1987), lake models such as MyLake (Saloranta and Andersen, 2007) and Delft3D (Lesser et al., 2004), and aquifer models such as MODFLOW-MT3D (Harbaugh, 2005; Bedekar et al., 2016) and FEFLOW (Trefry and Muffels, 2007), require the characterization of both horizontal and vertical boundary conditions because they do not represent entire closed systems such a river basin. Instead, they focus on sub-regions within such closed systems. On the other hand, catchment models such as INCA (Jackson-Blake et al., 2016; Wade et al., 2002; Whitehead et al., 1998) and SWAT (Arnold et al., 2012) only require vertical boundary conditions (e.g., precipitation) because they focus on the larger closed system that contains the entire basin area. Accordingly, these two scales of models tend to focus on different pollution problems. Sub-catchment models tend to focus more on point sources, such as wastewater discharge, and catchment models often look at diffuse pollution (e.g., agriculture nutrients and fertilizer use). These differences also result in different chemical species and biogeochemical cycles of focus, e.g., river models often address problems related to low Dissolved Oxygen (DO) levels caused by biomass decomposition and BOD (Biological Oxygen Demand) arising from wastewater discharges and other point sources discharging directly in river and lakes. OpenWQ enables multi-scale chemistry simulations that can be integrated into hydro-models of sub-catchment and catchment scales; thus, it can help bridge the gap between these two approaches, as well as allow for better integration of cross-dependent biogeochemical cycles. For example, whereas the DO and nitrogen cycles are often simulated in river-reach models, catchment models tend to focus more on the nitrogen cycle and assume that there is an unlimited amount of DO available. Although this assumption could be considered valid in many cases for surface runoff, it is certainly erroneous for water bodies such as rivers, lakes, and groundwater.

2. *Simple versus detailed biogeochemistry representation.* Water quality modeling tools have been developed with varying degrees of detail in the representation of biogeochemical processes (Costa et al., 2020a). For example, while INCA and HYPE (Lindström et al., 2010) provide simpler biogeochemical modeling approaches for the nitrogen and phosphorous cycles, requiring a smaller number of reaction-kinetic parameters to calibrate them may be more suitable for data-scarce
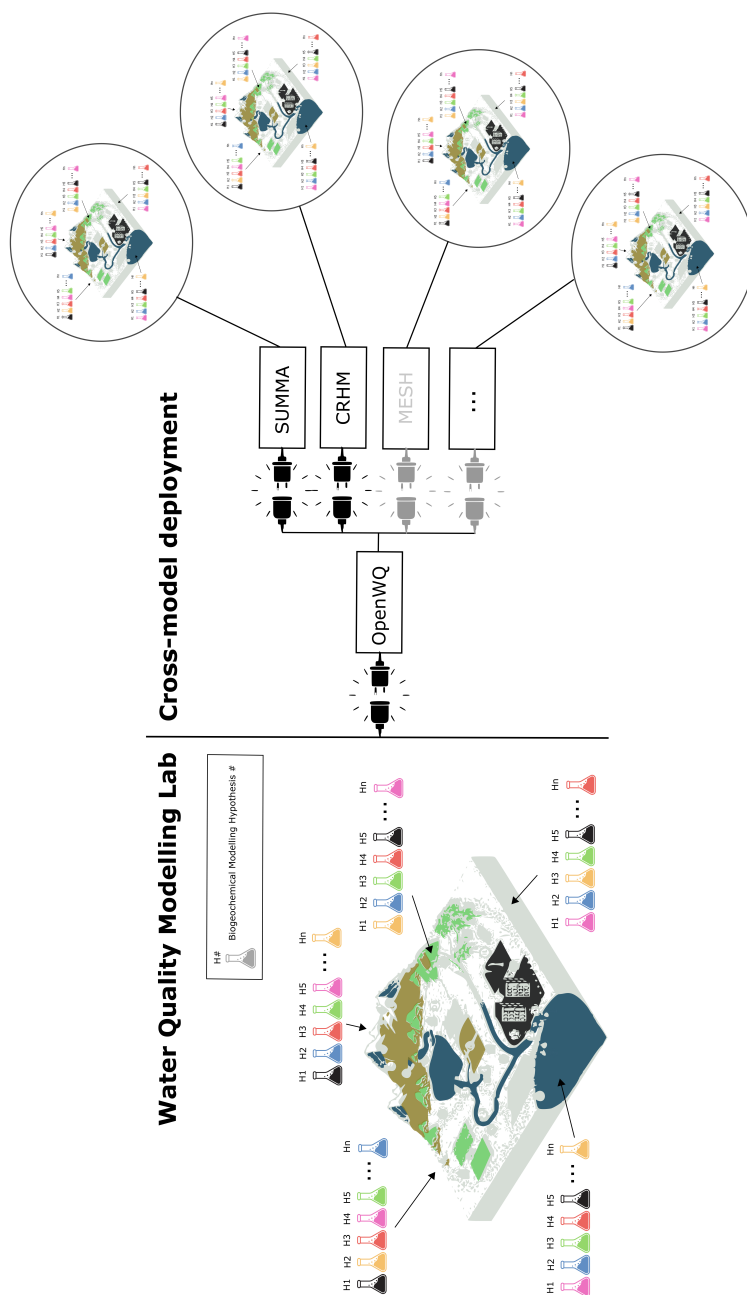
Figure 11. Cross-model deployment of biogeochemistry modeling setup, hypothesis and scenarios

365   regions; more complex biogeochemical models like HSPF (Bic, 1997) arguably provide higher model fidelity but may only be applicable in data-rich environments. However, when selecting a model for a particular region, modelers often have to make compromises with process representation because some models have more detailed physics-based coupled water-energy balance computations such as AnnAGNPS (Bosch et al., 1998) but may offer more limited biogeochemical capabilities (Costa et al., 2020a). OpenWQ enables addressing this issue through its flexible eco-modeling lab, which

370   allows testing different biogeochemical conceptual models and modeling hypotheses, from simple biogeochemical cycles and transformations to more complex and intertwined reaction networks involving dozens or hundreds of chemical species.

3. *Unconnected versus interconnected biogeochemical cycling representation.* Most catchment models simulate biogeo-

375   chemical cycles in isolation. For example, popular models such as SWAT and HYPE simulate the phosphorous and nitrogen cycles without integrating them with the DO-BOD cycle, despite them being strongly interrelated because DO is used in both cycles. In the nitrogen cycle, DO is used in nitrification, where ammonia is oxidized into nitrite (NO_3) and nitrate (NO_2). In the DO-BOD cycle, DO is used in the biological, aerobic decomposition of organic matter. OpenWQ aims to allow for a biogeochemistry representation that is less compartmentalized, making interactions between cycling

380   frameworks more fluid, flexible, and potentially closer to reality (i.e., model fidelity). In practice, DO dynamics affect the cycling of many chemical constituents, from nutrients to heavy metals. OpenWQ's eco-modeling lab addresses this issue through its open reaction-network solver, which provides the flexibility to deploy any number of biogeochemical cycling representations of any number of chemical species simultaneously, which can be connected or unconnected.

385   4. *Background chemical transport driver.* Typically, hydro-models are developed and maintained by research communities with specific research motivations driven by a regional context. These modeling tools often become highly specialized for particular environments and applications, and modelers commonly find it hard to find a water quality modeling tool that integrates such regionally important hydro-transport modeling capabilities. There is also in-house expertise that is passed on over the years between members of such communities and research groups, which can make them reluctant

390   to switch to other modeling tools because it may involve steep learning curves. OpenWQ aims to address this issue by enabling extension to water quality modeling capabilities directly on those models so that modelers can continue using the hydro-modeling tool that they consider more suitable to the environments on which they focus.

6.3   Limitations

1. *Dependency on accuracy of hydro-model flux calculations:* The physical transport of chemical constituents in OpenWQ

395   relies on the quality of the water fluxes passed by the host hydro-model. Although this may be an advantage since it allows choosing the hydro-model that best suits the modeling needs, it can become an issue if the calculated fluxes in the hydro-model are not accurate, e.g., see the issues highlighted by Woldegiorgis et al. (2023). Modelers should select the

hydro-model coupled to OpenWQ that is the most suitable for the application at hand or pursue the coupling of OpenWQ to another hydro-model.

400   2. *Biogeochemistry based on reaction networks*: The native biogeochemistry module of OpenWQ that provides water quality-lab capabilities assumes that biogeochemical cycling can be represented via a series of sequential and parallel reaction networks. Although this representation is true for most chemical constituents, pollution problems, and environmental studies, some biogeochemistry may involve formulations that rely on variable dependencies that may not be available in a particular coupled model. For example, simulating microbiological pollution in lakes, rivers, and beaches,

405   such as contamination with fecal coliforms originating from leaking septic tanks and wastewater discharges, requires the simulation of die-off rates due to exposure to solar radiation. In the case of hydrodynamic models, such information may not be available. In the case of hydrological models, which typically deal with such data, that variable dependency may not have been passed into OpenWQ during the coupling procedure, so updates to the coupler may be needed. OpenWQ's coupler functions have been designed to make the addition of new dependency variables straightforward. The portability

410   of OpenWQ is materialized through a series of coupler functions and wrapper interface functions that enable its coupling to hydro-models written in C++ or Fortran. However, the use of a more standardized model interface framework, such as the Basic Model Interface (BMI Peckham et al., 2013; Hutton et al., 2020), could help streamline further the coupling process through the use of standard control and query functions. This could make that model both easier to learn and easier to couple with other software elements. BMI, for example, currently supports five languages: C, C++, Fortran,

415   Java, and Python.

3. *Testing based on simple perturbation experiments*: The work presented here represents the first application of OpenWQ to improve water quality modeling, but there are many additional opportunities to build on this work. The case studies simulated here cover a range of pollution problems and hydrologic processes, but they are naturally limited in terms of the environments and contamination problems covered. The model simulations presented are also based on simple per-

420   turbation experiments, which were necessary for validation purposes; however, more comprehensive model applications should be carried out in the future for comparison with competing modeling approaches. The work presented also does not examine different numerical integration options. Research is needed to continue exploring the potential opportunities that OpenWQ creates for testing different biogeochemical, biophysical, and hydrologic processes and their model representations.

425   7   Conclusions

This paper describes OpenWQ as a methodology for the cross-model deployment of flexible multi-biogeochemistry simulations in existing process-based hydro-modeling tools. OpenWQ's concept was demonstrated through integration with two hydro-models, SUMMA and CRHM, and testing of pollution scenarios. The key points of this paper are as follows:

1. *Interoperability and coupling process*: Demonstration of coupling of OpenWQ to CRHM and SUMMA illustrates how

430   the coupling "recipe" presented can be deployed to link OpenWQ to hydro-models even if displaying different data

and model structures and/or programming languages. The coupling steps, coupling functions, and wrapper interface functions have been designed to optimize the coupling process.

2. *Flexibility, transparency and reproducibility*: The model development and applications presented illustrate how OpenWQ's flexible multi-chemistry lab capabilities enable addressing a variety of environmental and pollution problems, increasing model flexibility, transparency and reproducibility, as well as enabling comparing modeling hypotheses in a controlled manner.

3. *Controlled testing of modeling hypotheses*: The model applications presented aim to illustrate how biogeochemical modeling frameworks designed in OpenWQ can be readily deployed across different hydro-models using the same input files. This is extremely useful to promote the transfer of knowledge and enable the selection of the most appropriate background hydro-model for each situation based on landscape and climate considerations.

4. *Separating the numerical solver from the physicochemical calculations*. This separation enables more controlled simulations where the specific impacts of different process modules and numerical implementations can not only be properly quantified but also added or removed as needed for structural uncertainty characterization. Such model architecture is critical for model scalability.

The motivation for this development recognizes that (1) hydrology has a strong impact on the fate of pollution in the environment, but hydrological and water quality model developments often occur in isolation, (2) more should be done to facilitate collaboration between the hydrological and biogeochemical communities, (3) interoperability, transparency, flexibility, and reproducibility is needed to optimize research efforts and increase trust in model predictions. We look forward to continuing further developing and innovating in flexible and extensible water quality tools that are agnostic to the choice of the host hydro-model.

Code availability. The source code of OpenWQ and all support pre-processing and post-processing scripts are available in GitHub at https://github.com/ue-hydro/openwq and publish in Zenodo athttps://zenodo.org/records/10045291

Sample availability. The test cases used to validate OpenWQ are available in GitHub at https://github.com/ue-hydro/synthetic_tests. This repository includes the model figuration data for OpenWQ, SUMMA and CRHM, as well as post-processing scripts for replication of the results.

Appendix A: Deriving analytical solutions

Here, we provide details about the derivation of the analytical solutions used to verify the performance of OpenWQ. For each test, the final analytical solution is first provided and supported by a diagram describing the corresponding reaction network. The diagrams are then used to define the governing equations, which can be ordinary or partial differential equations.

A1 Tests 1 and 2 - Single-species batch reaction

Governing equations

The single-species batch reactor tests involve (a) first-order and (b) second-order decay kinetics. Fig. A1 depicts the biogeochemical process.
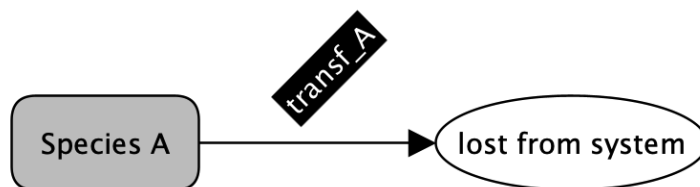
Figure A1. Single-species reaction network where transf_A is a first-order biogeochemical decay reaction.

The governing equation for a single species subject to first-order decay is given by Eq. A1. In turn, the governing equation for a single species subject to second-order is given by Eq. A2.

$$\frac{dc_A}{dt} = -kc_A, \tag{A1}$$

$$\frac{dc_A}{dt} = -kc_A^2. \tag{A2}$$

Analytical solutions

The analytical solution of a single species subject to first-order decay can be obtained by integrating Eq. A1. In turn, the analytical solution of a single species subject to second-order decay can be obtained by integrating Eq. A2.

$$\frac{dc_A}{dt} = -kc_A \Leftrightarrow \frac{1}{c_A}dc_A = -kdt \Leftrightarrow$$

$$\int_0^t \frac{1}{c_A}dc_A = \int_0^t -kdt \Leftrightarrow \ln(c_A)\Big|_0^t = -kt\Big|_0^t \Leftrightarrow$$

$$\ln(c_A(t)) - \ln(c_A(0)) = -k\Delta t \Leftrightarrow \ln\left(\frac{c_A(t)}{c_A(0)}\right) = -k\Delta t \Leftrightarrow$$

$$\frac{c_A(t)}{c_A(0)} = -k\Delta t \Leftrightarrow c_A(t) = c_A(0)e^{-k\Delta t}. \tag{A3}$$

475
$$\frac{dc_A}{dt} = -kc_A^2 \Leftrightarrow \frac{1}{c_A^2}dc_A = -kdt \Leftrightarrow$$

$$\int_0^t c_A^{-2}dc_A = \int_0^t -kdt \Leftrightarrow -c_A^{-1}\bigg|_0^t = -kt\bigg|_0^t \Leftrightarrow$$

$$c_A^{-1}\bigg|_0^t = kt\bigg|_0^t \Leftrightarrow c_A(t)^{-1} - c_A(0)^{-1} = k\Delta t \Leftrightarrow$$

$$\frac{1}{c_A(t)} = \frac{1}{c_A(0)} + k\Delta t \Leftrightarrow c_A(t) = \frac{1}{\dfrac{1}{c_A(0)} + k\Delta t}. \tag{A4}$$

A2 Test 3 - Two-species reaction network

480 **Governing equations**

The two-species reaction network with linear decay is represented schematically in Fig. A2.
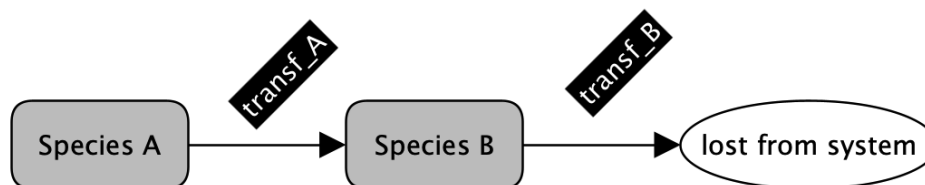
Figure A2. Two-species reaction network where transf_A and transf_B are first-order biogeochemical transformations.

The fate of Species A in a two-species reaction network only depends on its own concentration, so the governing equation is similar to that of the previous case, Eq. A1. However, the fate of Species B depends on the time evolution of concentrations of both Species A and B. The governing equation becomes

485
$$\frac{dc_B}{dt} = k_A c_A - k_B c_B. \tag{A5}$$

Analytical solutions

The analytical solutions for Species A is the same as in the previous case, which has been derived in Eq. A3. For Species B, to derive the analytical solution of Eq. A5, we can start by replacing $c_A(t)$ in Eq. A5 by its analytical solution obtained previously in Eq. A3. We obtain

490
$$\frac{dc_B}{dt} = k_A c_A(0)e^{-k_A t} - k_B c_B(t) \Leftrightarrow$$

$$\frac{dc_B}{dt} + k_B c_B = k_A c_A(0)e^{-k_A t}. \tag{A6}$$

The integrating factor, $e^{k_B t}$, can be used to integrate Eq. A6 by parts (i.e., $d(uv) = udv + vdu$). Multiplying Eq. A6 by the integrating factor, we obtain

$$\frac{dc_B}{dt}e^{k_B t} + k_B c_B(t)e^{k_B t} = k_A c_A(0)e^{-k_A t}e^{k_B t} \Leftrightarrow$$

495
$$\frac{dc_B}{dt}e^{k_B t} + k_B c_B(t)e^{k_B t} = k_A c_A(0)e^{(k_B - k_A)t}. \tag{A7}$$

Using the general expression for integration by parts and considering that functions u and v are given by $u = c_B$ and $v = e^{k_B t}$, we obtain

$$d\left(c_B e^{k_B t}\right) = c_B d\left(e^{k_B t}\right) + e^{k_B t} dc_B. \tag{A8}$$

Replacing the derivative of $e^{k_B t}$ in Eq. A8, where $d\left(e^{k_B t}\right) = k_B e^{k_B t} dt$, leads to

500
$$d(uv) = udv + vdu \Leftrightarrow$$
$$d\left(c_B e^{k_B t}\right) = c_B\left(k_B e^{k_B t} dt\right) + e^{k_B t} dc_B, \tag{A9}$$

or

$$\frac{d}{dt}\left(c_B e^{k_B t}\right) = c_B k_B e^{k_B t} + e^{k_B t}\frac{dc_B}{dt}. \tag{A10}$$

The right-hand side of Eq. A10 is the same as the left-hand side of Eq. A7, so the same applies to the other side of the
505 equations. Thus, we can re-write the equations as

$$\frac{d}{dt}\left(c_B e^{k_B t}\right) = k_A c_A(0)e^{(-k_A t)}e^{k_B t} \Leftrightarrow$$
$$\frac{d}{dt}\left(c_B e^{k_B t}\right) = k_A c_A(0)e^{(k_B - k_A)t} \Leftrightarrow$$
$$d\left(c_B e^{k_B t}\right) = k_A c_A(0)e^{(k_B - k_A)t} dt. \tag{A11}$$

Integrating both sides of the equation, we obtain

510
$$\int_0^t d(c_B e^{k_B t}) = \int_0^t k_A c_A(0)e^{(k_B - k_A)t} dt \Leftrightarrow$$

$$c_B(t)e^{k_B t} = \frac{k_A c_A(0)}{k_B - k_A}e^{(k_B - k_A)t} + C', \tag{A12}$$

where C' is the integration constant. At $t = 0$, Eq. A12 can be written as

$$c_B(0)e^0 = \frac{k_A c_A(0)}{k_B - k_A}e^0 \Leftrightarrow$$

$$C' = c_B(0) - \frac{k_A c_A(0)}{k_B - k_A}, \tag{A13}$$

which can be replaced in Eq. A12 to give

$$c_B(t)e^{k_B t} = \frac{k_A c_A(0)}{k_B - k_A}e^{(k_B - k_A)t} + c_B(0) - \frac{k_A c_A(0)}{k_B - k_A} \Leftrightarrow$$

$$c_B(t)e^{k_B t} = \frac{k_A c_A(0)}{k_B - k_A}\left(e^{(k_B - k_A)t} - 1\right) + c_B(0) \Leftrightarrow$$

$$c_B(t) = \frac{k_A c_A(0)}{k_B - k_A}\left(\frac{e^{(k_B - k_A)t}}{e^{k_B t}} - \frac{1}{e^{k_B t}}\right) + \frac{c_B(0)}{e^{k_B t}} \Leftrightarrow$$

$$c_B(t) = \frac{k_A c_A(0)}{k_B - k_A}\left(e^{-k_A t} - e^{-k_B t}\right) + c_B(0)e^{-k_B t}. \tag{A14}$$

A3 Test 4 - Three-species reaction network

Governing equations

The three-species reaction network with linear decay is represented schematically in Fig. A2.
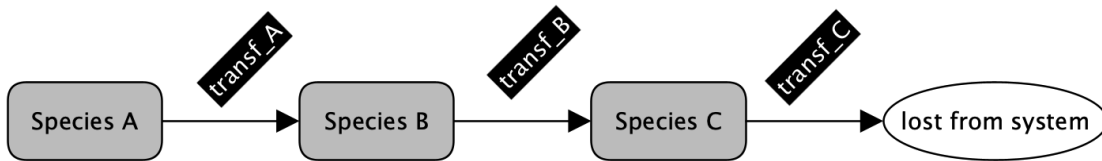
Figure A3. Three-species reaction network where transf_A, transf_B, and transf_C are first-order biogeochemical transformations.

The governing equations for Species A and B are similar to the previous cases, Eqs. A1 and A5, respectively. The governing equation for Species C can be written as

$$\frac{dc_C}{dt} = k_B c_B - k_C c_C. \tag{A15}$$

Analytical solutions

The analytical solutions for Species A is the same as in the previous case, which has been derived in Eq. A3. Similarly, the analytical solutions for Species B has been derived in Eqs. A6 through Eq. A14. The analytical solution for Species C can be derived by first substituting $c_B(t)$ in Eq. A15 by Eq. A14 to obtain

530
$$\frac{dc_C}{dt} = k_B \left(\frac{k_A c_A(0)}{k_B - k_A} \left[e^{-k_A t} - e^{-k_B t} \right] + c_B(0) e^{-k_B t} \right) - k_C c_C \Leftrightarrow$$

$$\frac{dc_C}{dt} + k_C c_C = k_B \left(\frac{k_A c_A(0)}{k_B - k_A} \left[e^{-k_A t} - e^{-k_B t} \right] + c_B(0) e^{-k_B t} \right). \tag{A16}$$

The integrating factor used in Appendix A2 to enable integration of parts, $e^{k_C t}$, can be used here as well. Multiplying Eq. A16 by this integrating factor, we obtain

$$\frac{dc_C}{dt} e^{k_C t} + k_C c_C(t) e^{k_C t} = k_B \left(\frac{k_A c_A(0)}{k_B - k_A} \left[e^{-k_A t} - e^{-k_B t} \right] + c_B(0) e^{-k_B t} \right) e^{k_C t}. \tag{A17}$$

535 We can use the same expression derived to enable integration by parts in the previous case (Eq. A10) but replacing Species B by Species C: $\frac{d}{dt} \left(c_C e^{k_C t} \right) = c_C k_C e^{k_C t} + \frac{dc_C}{dt} e^{k_C t}$. Also, similarly to the previous case, the right-hand side of this equation is the same as the left-hand side of Eq. A17, so the same applies to the other side of the equations. Thus, we can re-write the equations as

$$\frac{d}{dt} \left(c_C e^{k_C t} \right) = k_B \left(\frac{k_A c_A(0)}{k_B - k_A} \left[e^{-k_A t} - e^{-k_B t} \right] + c_B(0) e^{-k_B t} \right) e^{k_C t} \Leftrightarrow$$

540
$$d \left(c_C e^{k_C t} \right) = k_B \left(\frac{k_A c_A(0)}{k_B - k_A} \left[e^{-k_A t} - e^{-k_B t} \right] + c_B(0) e^{-k_B t} \right) e^{k_C t} dt \Leftrightarrow$$

$$d \left(c_C e^{k_C t} \right) = k_B \left(\frac{k_A c_A(0)}{k_B - k_A} \left[e^{(k_C - k_A)t} - e^{(k_C - k_B)t} \right] + c_B(0) e^{(k_C - k_B)t} \right) dt. \tag{A18}$$

Integrating both sides of the equation, we obtain

$$\int_0^t d \left(c_C e^{k_C t} \right) = \int_0^t \left[k_B \left(\frac{k_A c_A(0)}{k_B - k_A} \left[e^{(k_C - k_A)t} - e^{(k_C - k_B)t} \right] + c_B(0) e^{(k_C - k_B)t} \right) \right] \Leftrightarrow$$

$$c_C(t) e^{k_C t} = k_B \left(\frac{k_A c_A(0)}{k_B - k_A} \left[\frac{1}{k_C - k_A} e^{(k_C - k_A)t} - \frac{1}{k_C - k_B} e^{(k_C - k_B)t} \right] + \frac{c_B(0)}{k_C - k_B} e^{(k_C - k_B)t} \right) + C'', \tag{A19}$$

545 where C'' is the integration constant. At $t = 0$, Eq. A19 becomes

$$c_C(0)e^{(k_C 0)} = k_B\left(\frac{k_A c_A(0)}{k_B - k_A}\left[\frac{1}{k_C - k_A}e^0 - \frac{1}{k_C - k_B}e^{(k_C - k_B)0}\right] + \frac{c_B(0)}{k_C - k_B}e^0\right) + C'' \Leftrightarrow$$

$$c_C(0)1 = k_B\left(\frac{k_A c_A(0)}{k_B - k_A}\left[\frac{1}{k_C - k_A}1 - \frac{1}{k_C - k_B}1\right] + \frac{c_B(0)}{k_C - k_B}1\right) + C'' \Leftrightarrow$$

$$C'' = c_C(0) - k_B\left(\frac{k_A c_A(0)}{k_B - k_A}\left[\frac{1}{k_C - k_A} - \frac{1}{k_C - k_B}\right] + \frac{c_B(0)}{k_C - k_B}\right), \tag{A20}$$

which can be replaced in Eq. A19 to give

$$c_C(t)e^{k_C t} = k_B\left(\frac{k_A c_A(0)}{k_B - k_A}\left[\frac{1}{k_C - k_A}e^{(k_C - k_A)t} - \frac{1}{k_C - k_B}e^{(k_C - k_B)t}\right] + \frac{c_B(0)}{k_C - k_B}e^{(k_C - k_B)t}\right)$$
$$+ c_C(0) - k_B\left(\frac{k_A c_A(0)}{k_B - k_A}\left[\frac{1}{k_C - k_A} - \frac{1}{k_C - k_B}\right] + \frac{c_B(0)}{k_C - k_B}\right). \tag{A21}$$

This can be rearranged to give

$$c_C(t) = k_B\left(\frac{k_A c_A(0)}{k_B - k_A}\left[\frac{1}{k_C - k_A}e^{-k_A t} - \frac{1}{k_C - k_B}e^{-k_B t}\right] + \frac{c_B(0)}{k_C - k_B}e^{-k_B t}\right) + c_C(0)e^{-k_C t}$$
$$- k_B\left(\frac{k_A c_A(0)}{k_B - k_A}\left[\frac{1}{k_C - k_A} - \frac{1}{k_C - k_B}\right] + \frac{c_B(0)}{k_C - k_B}\right)e^{-k_C t}, \tag{A22}$$

and then simplified to

$$c_C(t) = k_B\left(\frac{k_A c_A(0)}{k_B - k_A}\left[\frac{e^{-k_A t}}{k_C - k_A} - \frac{e^{-k_B t}}{k_C - k_B}\right] + \frac{c_B(0)e^{-k_B t}}{k_C - k_B}\right) + c_C(0)e^{-k_C t}$$
$$- k_B\left(\frac{k_A c_A(0)}{k_B - k_A}\left[\frac{e^{-k_C t}}{k_C - k_A} - \frac{e^{-k_C t}}{k_C - k_B}\right] + \frac{c_B(0)e^{-k_C t}}{k_C - k_B}\right). \tag{A23}$$

A4   Test 5 - Nitrogen cycle

Governing equations

The simulation of the nitrogen cycle is common in freshwater water quality studies because it allows addressing pollution problems related to nutrient excess and eutrophication. Typical conceptual models used for the nitrogen cycle involve several nitrogen species, such as depicted in Fig. A4. This particular conceptual model is similar to that used in several catchment-scale models like SWAT (Arnold et al., 2012), HYPE (Lindström et al., 2010), INCA (WHI, 1998), and CRHM-WQ (Costa et al., 2021) models. The nitrogen-cycle test performed with OpenWQ in this paper is based on this particular conceptual model because it is a popular one. Yet, it should be noted that OpenWQ was designed to allow flexibly changing it and comparing different conceptual models and modelling hypotheses.
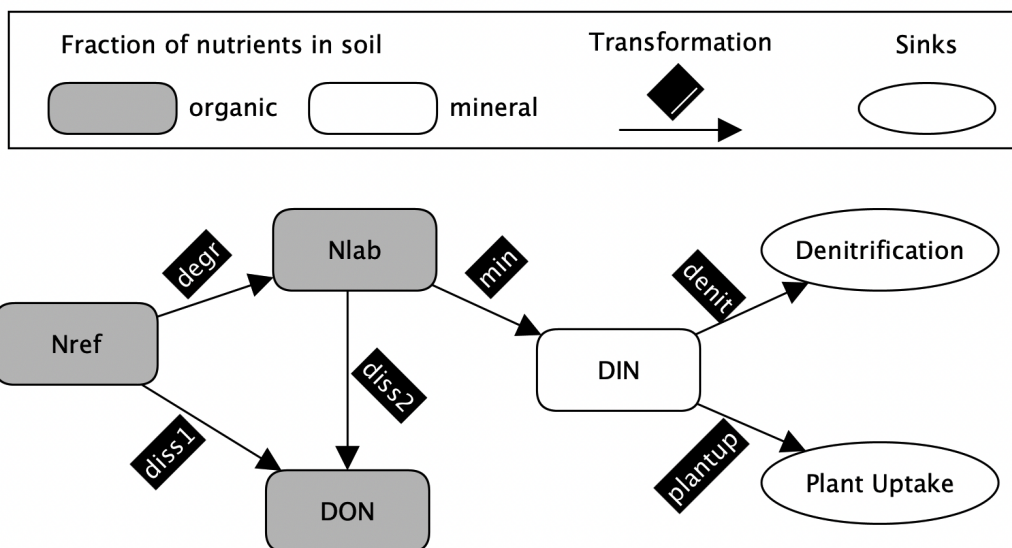
Figure A4. Nitrogen cycle as represented in several popular catchment-scale models. The nitrogen species Nref refers to refractory nitrogen, Nlab refers to labile nitrogen, DON refers to dissolved organic nitrogen, and DIN refers to dissolved innorganic nitrogen. The transformation degr refers to degration; diss1 and diss2 refers to dissolution from Nref and Nlab, respectively; min refers to mineralization; denitr refers to denitrification; and plantup refers to plant uptake.

The governing equations for the different N species are similar to those presented before but need to be re-written here because they are integrated within a more intricate reaction network that gives rise to more variable dependences; therefore, requiring new derivations in some cases. The governing equations for Nref, Nlab, DON, and DIN are given by Eqs. A24, A25,
570 A26, and A27, respectively.

$$\frac{dc_{\mathrm{Nref}}}{dt} = -(k_{\mathrm{degr}} + k_{\mathrm{diss1}})c_{\mathrm{Nref}}, \tag{A24}$$

$$\frac{dc_{\mathrm{Nlab}}}{dt} = k_{\mathrm{degr}}c_{\mathrm{Nref}} - (k_{\mathrm{min}} + k_{\mathrm{diss1}})c_{\mathrm{Nlab}}, \tag{A25}$$

$$\frac{dc_{\mathrm{DON}}}{dt} = k_{\mathrm{diss1}}c_{\mathrm{Nref}} + k_{\mathrm{diss2}}c_{\mathrm{Nlab}}, \tag{A26}$$

$$\frac{dc_{\mathrm{DIN}}}{dt} = k_{\mathrm{min}}c_{\mathrm{Nlab}} - (k_{\mathrm{denit}} + k_{\mathrm{plantup}})c_{\mathrm{DIN}}. \tag{A27}$$

575 **Analytical solutions**

The derivation of the analytical solutions for the different nitrogen species depends on the positioning of the various species in the reaction chain.

1. **refractoryN** (Nref): The solution is similar to that derived in Eq. A3, which reads as follows when adapted to the specific N cycle considered here:

$$c_{\mathrm{Nref}}(t) = c_{\mathrm{Nref}}(0)e^{-(k_{\mathrm{degr}}+k_{\mathrm{diss1}})t}. \tag{A28}$$

2. **labileN** (Nlab): The solution is similar to that derived in Eq. A14, which reads as follows when adapted to the specific N cycle considered here:

$$c_{\mathrm{Nlab}}(t) = \frac{k_{\mathrm{degr}}c_{\mathrm{Nref}}(0)}{k_{\mathrm{min}}+k_{\mathrm{diss2}}-k_{\mathrm{degr}}}\left(e^{-k_{\mathrm{degr}}t}-e^{-(k_{\mathrm{min}}+k_{\mathrm{diss2}})t}\right) + c_{\mathrm{Nlab}}(0)e^{-(k_{\mathrm{min}}+k_{\mathrm{diss2}})t}. \tag{A29}$$

3. **DON** The concentration of DON does not depend on itself, but rather on the evolution of Nref and Nlab. Analytical solutions suitable for c_{Nref} and c_{Nlab} have been provided above in Eqs. A28 and A29, respectively. These solutions can be substituted into Eq. A26 as follows:

$$\frac{dc_{\mathrm{DON}}}{dt} = k_{\mathrm{diss1}}c_{\mathrm{Nref}}e^{-(k_{\mathrm{degr}}+k_{\mathrm{diss1}})t} + k_{\mathrm{diss2}}\left[\frac{k_{\mathrm{degr}}c_{\mathrm{Nref}}}{k_{\mathrm{min}}+k_{\mathrm{diss2}}-k_{\mathrm{degr}}}\left(e^{-k_{\mathrm{degr}}t}-e^{-(k_{\mathrm{min}}+k_{\mathrm{diss2}})t}\right)\right.$$
$$\left. + \; c_{\mathrm{Nlab}}(0)e^{-(k_{\mathrm{min}}+k_{\mathrm{diss2}})t}\right]. \tag{A30}$$

Because this solution is independent of the concentration of DON, it can be integrated in its current state.

$$dc_{\mathrm{DON}} = k_{\mathrm{diss1}}c_{\mathrm{Nref}}e^{-(k_{\mathrm{degr}}+k_{\mathrm{diss1}})t}dt + k_{\mathrm{diss2}}\left[\frac{k_{\mathrm{degr}}c_{\mathrm{Nref}}}{k_{\mathrm{min}}+k_{\mathrm{diss2}}-k_{\mathrm{degrd}}}\left(e^{-k_{\mathrm{degr}}t}-e^{-(k_{\mathrm{min}}+k_{\mathrm{diss2}})t}\right)\right.$$
$$\left. +c_{\mathrm{Nlab}}(0)e^{-(k_{\mathrm{min}}+k_{\mathrm{diss2}})t}\right]dt \Leftrightarrow$$

$$c_{\mathrm{DON}}(t) = \frac{k_{\mathrm{diss1}}c_{\mathrm{Nref}}(t)}{-(k_{\mathrm{degr}}+k_{\mathrm{diss1}})}e^{-(k_{\mathrm{degr}}+k_{\mathrm{diss1}})t} + \frac{k_{\mathrm{diss2}}k_{\mathrm{degr}}c_{\mathrm{Nref}}(t)}{k_{\mathrm{min}}+k_{\mathrm{diss2}}-k_{\mathrm{degr}}}\left(\frac{e^{-k_{\mathrm{degr}}t}}{-k_{\mathrm{degr}}}-\frac{e^{-(k_{\mathrm{min}}+k_{\mathrm{diss2}})t}}{-(k_{\mathrm{min}}+k_{\mathrm{diss2}})}\right)$$
$$+\frac{k_{\mathrm{diss2}}c_{\mathrm{Nlab}}(0)}{-(k_{\mathrm{min}}+k_{\mathrm{diss2}})}e^{-(k_{\mathrm{min}}+k_{\mathrm{diss2}})t} + C'''. \tag{A31}$$

Considering that at $t = 0$, $c_{\mathrm{DON}}(t)$ becomes $c_{\mathrm{DON}}(0)$, we can determine C''' as

$$C''' = c_{\mathrm{DON}}(0) + \frac{k_{\mathrm{diss1}}c_{\mathrm{Nref}}(t)}{k_{\mathrm{degr}}+k_{\mathrm{diss1}}} - \frac{k_{\mathrm{diss2}}k_{\mathrm{degr}}c_{\mathrm{Nref}}(t)}{k_{\mathrm{min}}+k_{\mathrm{diss2}}-k_{\mathrm{degr}}}\left(\frac{1}{-k_{\mathrm{degr}}}-\frac{1}{-(k_{\mathrm{min}}+k_{\mathrm{diss2}})}\right) + \frac{k_{\mathrm{diss2}}c_{\mathrm{Nlab}}(0)}{-(k_{\mathrm{min}}+k_{\mathrm{diss2}})}. \tag{A32}$$

Replacing Eq. A32 into Eq. A31 we obtain

$$c_{\text{DON}}(t) = \frac{k_{\text{diss1}} c_{\text{Nref}}(t)}{-(k_{\text{degr}} + k_{\text{diss1}})} e^{-(k_{\text{degr}}+k_{\text{diss1}})t} + \frac{k_{\text{diss2}} k_{\text{degr}} c_{\text{Nref}}(t)}{k_{\text{min}} + k_{\text{diss2}} - k_{\text{degr}}} \left(\frac{e^{-k_{\text{degr}}t}}{-k_{\text{degr}}} - \frac{e^{-(k_{\text{min}}+k_{\text{diss2}})t}}{-(k_{\text{min}} + k_{\text{diss2}})} \right)$$

$$+ \frac{k_{\text{diss2}} c_{\text{Nlab}}(0)}{-(k_{\text{min}} + k_{\text{diss2}})} e^{-(k_{\text{min}}+k_{\text{diss2}})t} + c_{\text{DON}}(0) + \frac{k_{\text{diss1}} c_{\text{Nref}}(t)}{k_{\text{degr}} + k_{\text{diss1}}} - \frac{k_{\text{diss2}} k_{\text{degr}} c_{\text{Nref}}(t)}{k_{\text{min}} + k_{\text{diss2}} - k_{\text{degr}}} \left(\frac{1}{-k_{\text{degr}}} \right.$$

$$\left. - \frac{1}{-(k_{\text{min}} + k_{\text{diss2}})} \right) + \frac{k_{\text{diss2}} c_{\text{Nlab}}(0)}{-(k_{\text{min}} + k_{\text{diss2}})} \,. \tag{A33}$$

Eq. A33 can be simplified to obtain

$$c_{\text{DON}}(t) = -\frac{k_{\text{diss1}} c_{\text{Nref}}(t)}{k_{\text{degr}} + k_{\text{diss1}}} e^{-(k_{\text{degr}}+k_{\text{diss1}})t} + \frac{k_{\text{diss2}} k_{\text{degr}} c_{\text{Nref}}(t)}{k_{\text{min}} + k_{\text{diss2}} - k_{\text{degr}}} \left(\frac{e^{(k_{\text{min}}+k_{\text{diss2}})t}}{k_{\text{min}} + k_{\text{diss2}}} - \frac{e^{-k_{\text{degr}}t}}{k_{\text{degr}}} \right)$$

$$- \frac{k_{\text{diss2}} c_{\text{Nlab}}(0)}{k_{\text{min}} + k_{\text{diss2}}} e^{-(k_{\text{min}}+k_{\text{diss2}})t} + c_{\text{DON}}(0) + \frac{k_{\text{diss1}} c_{\text{Nref}}(t)}{k_{\text{degr}} + k_{\text{diss1}}} - \frac{k_{\text{diss2}} k_{\text{degr}} c_{\text{Nref}}(t)}{k_{\text{min}} + k_{\text{diss2}} - k_{\text{degr}}} \left(\frac{1}{k_{\text{min}} + k_{\text{diss2}}} \right.$$

$$\left. - \frac{1}{k_{\text{degr}}} \right) - \frac{k_{\text{diss2}} c_{\text{Nlab}}(0)}{k_{\text{min}} + k_{\text{diss2}}} \,. \tag{A34}$$

4. **DIN**

The concentration of $c_{\text{Nlab}}(t)$ has been derived above in Eq. A29 and can be replaced in Eq. A27 to give

$$\frac{dc_{\text{DIN}}}{dt} = k_{\text{min}} \left[\frac{k_{\text{degr}} c_{(\text{Nref},0)}}{k_{\text{min}} + k_{\text{diss2}} - k_{\text{degr}}} \left(e^{-k_{\text{degr}}t} - e^{-(k_{\text{min}}+k_{\text{diss2}})t} \right) + c_{\text{Nlab}}(0) e^{-(k_{\text{min}}+k_{\text{diss2}})t} \right]$$

$$- (k_{\text{denit}} + k_{\text{plantup}}) c_{\text{DIN}}(t) \Leftrightarrow$$

$$\frac{dc_{\text{DIN}}}{dt} = \frac{k_{\text{min}} k_{\text{degr}} c_{(\text{Nref},0)}}{k_{\text{min}} + k_{\text{diss2}} - k_{\text{degr}}} \left(e^{-k_{\text{degr}}t} - e^{-(k_{\text{min}}+k_{\text{diss2}})t} \right) + k_{\text{min}} c_{\text{Nlab}}(0) e^{-(k_{\text{min}}+k_{\text{diss2}})t}$$

$$- (k_{\text{denit}} + k_{\text{plantup}}) c_{\text{DIN}} \,. \tag{A35}$$

The same integrating factor used before, which in this context reads $e^{(k_{\text{denit}}+k_{\text{plantup}})t}$, can be used here to allow similar integration by parts (i.e., $d(uv) = u\,dv + v\,du$). Multiplying Eq. A35 by the integration factor, we obtain

$$\frac{dc_{\text{DIN}}}{dt} e^{(k_{\text{denit}}+k_{\text{plantup}})t} + (k_{\text{denit}} + k_{\text{plantup}}) c_{\text{DIN}}(t) e^{(k_{\text{denit}}+k_{\text{plantup}})t}$$

$$= \frac{k_{\text{min}} k_{\text{degr}} c_{\text{Nref}}(0)}{k_{\text{min}} + k_{\text{diss2}} - k_{\text{degr}}} \left(e^{-k_{\text{degr}}t} - e^{-(k_{\text{min}}+k_{\text{diss2}})t} \right) e^{(k_{\text{denit}}+k_{\text{plantup}})t} + k_{\text{min}} c_{\text{Nlab}}(0) e^{-(k_{\text{min}}+k_{\text{diss2}})t} e^{(k_{\text{denit}}+k_{\text{plantup}})t} \,. \tag{A36}$$

Now we can use the same expression derived for integration by parts of previous cases (i.e., Eq. A10) and adapt it to DIN and the respective transformations:

$$\frac{d}{dt}\left(c_{\text{DIN}}e^{(k_{\text{denit}}+k_{\text{plantup}})t}\right) = \frac{dc_{\text{DIN}}}{dt}e^{(k_{\text{denit}}+k_{\text{plantup}})t} + (k_{\text{denit}}+k_{\text{plantup}})c_{\text{DIN}}e^{(k_{\text{denit}}+k_{\text{plantup}})t}. \tag{A37}$$

Similar to previous cases, the right-hand side of this equation is the same as the left-hand side of Eq. A35, so the same applies to the other side of the equations so that we can re-write the equations as

$$\frac{d}{dt}\left(c_{\text{DIN}}e^{(k_{\text{denit}}+k_{\text{plantup}})t}\right) = \frac{k_{\text{min}}k_{\text{degr}}c_{\text{Nref}}(0)}{k_{\text{min}}+k_{\text{diss2}}-k_{\text{degr}}}\left(e^{-k_{\text{degr}}t}-e^{-(k_{\text{min}}+k_{\text{diss2}})t}\right)e^{(k_{\text{denit}}+k_{\text{plantup}})t}$$

$$+k_{\text{min}}c_{\text{Nlab}}(0)e^{-(k_{\text{min}}+k_{\text{diss2}})t}e^{(k_{\text{denit}}+k_{\text{plantup}})t} \Leftrightarrow$$

$$d\left(c_{\text{DIN}}e^{(k_{\text{denit}}+k_{\text{plantup}})t}\right) = \left[\frac{k_{\text{min}}k_{\text{degr}}c_{\text{Nref}}(0)}{k_{\text{min}}+k_{\text{diss2}}-k_{\text{degr}}}\left(e^{(k_{\text{denit}}+k_{\text{plantup}}-k_{\text{degr}})t}-e^{(k_{\text{denit}}+k_{\text{plantup}}-k_{\text{min}}-k_{\text{diss2}})t}\right)\right.$$

$$\left.+k_{\text{min}}c_{\text{Nlab}}(0)e^{(k_{\text{denit}}+k_{\text{plantup}}-k_{\text{min}}-k_{\text{diss2}})t}\right]dt. \tag{A38}$$

Now we can integrate the equation with respect to $c_{\text{DIN}}(t)$ and t:

$$\int d\left(c_{\text{DIN}}e^{(k_{\text{denit}}+k_{\text{plantup}})t}\right) = \int \left[\frac{k_{\text{min}}k_{\text{degr}}c_{\text{Nref}}(0)}{k_{\text{min}}+k_{\text{diss2}}-k_{\text{degr}}}\left(e^{(k_{\text{denit}}+k_{\text{plantup}}-k_{\text{degr}})t}-e^{(k_{\text{denit}}+k_{\text{plantup}}-k_{\text{min}}-k_{\text{diss2}})t}\right)\right.$$

$$\left.+k_{\text{min}}c_{\text{Nlab}}(0)e^{(k_{\text{denit}}+k_{\text{plantup}}-k_{\text{min}}-k_{\text{diss2}})t}\right]dt \Leftrightarrow$$

$$c_{\text{DIN}}(t)e^{(k_{\text{denit}}+k_{\text{plantup}})t} = \frac{k_{\text{min}}k_{\text{degr}}c_{\text{Nref}}(0)}{k_{\text{min}}+k_{\text{diss2}}-k_{\text{degr}}}\left(\frac{e^{(k_{\text{denit}}+k_{\text{plantup}}-k_{\text{degr}})t}}{k_{\text{denit}}+k_{\text{plantup}}-k_{\text{degr}}}-\frac{e^{(k_{\text{denit}}+k_{\text{plantup}}-k_{\text{min}}-k_{\text{diss2}})t}}{k_{\text{denit}}+k_{\text{plantup}}-k_{\text{min}}-k_{\text{diss2}}}\right)$$

$$+k_{\text{min}}c_{\text{Nlab}}(0)\frac{e^{(k_{\text{denit}}+k_{\text{plantup}}-k_{\text{min}}-k_{\text{diss2}})t}}{k_{\text{denit}}+k_{\text{plantup}}-k_{\text{min}}-k_{\text{diss}}}+C''''. \tag{A39}$$

Considering that at $t=0$, $c_{\text{DIN}}(t)$ becomes $c_{\text{DIN}}(0)$, we can determine the constant C'''' as follows:

$$C'''' = c_{\text{DIN}}(0) - \frac{k_{\text{miner}}k_{\text{degr}}c_{\text{Nref}}(0)}{k_{\text{min}}+k_{\text{diss2}}-k_{\text{degr}}}\left(\frac{1}{k_{\text{denit}}+k_{\text{plantup}}-k_{\text{degr}}}-\frac{1}{k_{\text{denit}}+k_{\text{plantup}}-k_{\text{min}}-k_{\text{diss2}}}\right)$$

$$-k_{\text{miner}}c_{\text{Nlab}}(0)\frac{1}{k_{\text{denit}}+k_{\text{plantup}}-k_{\text{min}}-k_{\text{diss2}}}. \tag{A40}$$

Replacing the integrating constant in Eq. A39 we obtain

$$c_{\text{DIN}}(t)e^{(k_{\text{denit}}+k_{\text{plantup}})t} = \frac{k_{\min}k_{\text{degr}}c_{\text{Nref}}(0)}{k_{\min}+k_{\text{diss2}}-k_{\text{degr}}}\left(\frac{e^{(k_{\text{denit}}+k_{\text{plantup}}-k_{\text{degr}})t}}{k_{\text{denitr}}+k_{\text{plantup}}-k_{\text{degr}}} - \frac{e^{(k_{\text{denit}}+k_{\text{plantup}}-k_{\min}-k_{\text{diss2}})t}}{k_{\text{denit}}+k_{\text{plantup}}-k_{\min}-k_{\text{diss2}}}\right)$$

$$+k_{\min}c_{\text{Nlab}}(0)\frac{e^{(k_{\text{denit}}+k_{\text{plantup}}-k_{\min}-k_{\text{diss2}})t}}{k_{\text{denit}}+k_{\text{plantup}}-k_{\min}-k_{\text{diss2}}} + c_{\text{DIN}}(0) - \frac{k_{\min}k_{\text{degr}}c_{\text{Nref}}(0)}{k_{\min}+k_{\text{diss2}}-k_{\text{degr}}}\left(\frac{1}{k_{\text{denit}}+k_{\text{plantup}}-k_{\text{degr}}}\right.$$

$$\left.-\frac{1}{k_{\text{denit}}+k_{\text{plantup}}-k_{\min}-k_{\text{diss2}}}\right) - k_{\min}c_{\text{Nlab}}(0)\frac{1}{k_{\text{denit}}+k_{\text{plantup}}-k_{\min}-k_{\text{diss2}}} . \tag{A41}$$

A5 Test 6 - DO-BOD cycle

Governing equation

Dissolved oxygen (DO) depletion in rivers and lakes is a common consequence of pollution. It typically occurs near discharge outlets of untreated wastewater and can lead to high levels of organic matter that, during decomposition by aerobic bacteria, causes a DO sag in the water column. For the purposes of DO dynamics, such organic matter is typically translated into units of biological oxygen demand (BOD). Fig. A5 depicts the processes involved.
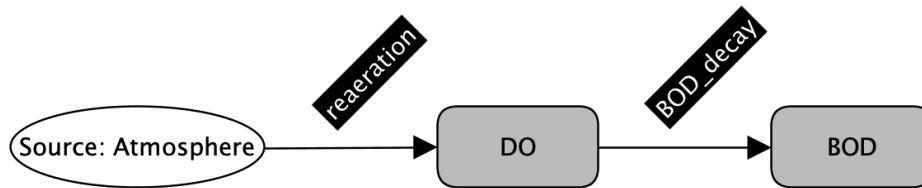
Figure A5. Representation of the transformations involved in the $BOD - DO$ cycle

The governing equation is the well known the Streeter–Phelps model (Streeter and Phelps, 1925). The equation states that the total rate of change in oxygen deficit (D) is equal to the difference between the two rates of deoxygenation and reaeration at any time, and it reads:

$$\frac{dD}{dt} = k_1 L_{\text{t}} - k_2 D, \tag{A42}$$

where D is the saturation deficit in g/m^3, which can be derived from the dissolved oxygen concentration at saturation minus the actual dissolved oxygen concentration ($D = DO_{\text{sat}} - DO$); k_1 is the deoxygenation rate, usually in d^{-1}; $L_{\text{t}} = L_{\text{a}}e^{-k_1 t}$; L_{a} is the initial oxygen demand of organic matter in the water, also called the ultimate BOD (BOD at time $t = \infty$); and k_2 is the reaeration rate, usually in d^{-1} . The unit of L_a is g/m^3; k_1; L_t is the oxygen demand remaining at time t, and t is the elapsed time, usually in days.

Analytical solutions equation

650 The solution has long been derived by Streeter and Phelps (1925) and it reads

$$D = \frac{k_1 L_a}{k_2 - k_1}\left(e^{-k_1 t} - e^{-k_2 t}\right) + D_a e^{-k_2 t}, \tag{A43}$$

where D_a is the initial oxygen deficit $[g/m^3]$.

A6 Tests 7 and 8 - Reactive and non-reactive transport with instantaneous point source

Governing equation

655 These tests were only performed with SUMMA-OpenWQ because OpenWQ's solute transport modules were only integrated in SUMMA-OpenWQ. They were not integrated in CRHM-OpenWQ because CRHM has its own solute transport routines (Costa et al., 2021). The general governing equation is the 1D diffusion-advection-reaction partial differential equation that is given by

$$\frac{\partial c}{\partial t} = D_x \frac{\partial^2 c}{\partial x^2} - \nu \frac{\partial c}{\partial x} - \lambda c, \tag{A44}$$

660 where c is the concentration of the tracer, t is time, D_x is the diffusion coefficient in the flow direction, x is the distance in the flow direction, ν is the flow velocity in the x-direction, and λ is a linear reaction term that can be set to zero for non-reactive tracers. However, this equation has been modified by Wexler (1992) for the scenario of an instantaneous point source, and it reads:

$$\frac{\partial c}{\partial t} = D_x \frac{\partial^2 c}{\partial x^2} - \nu \frac{\partial c}{\partial x} - \lambda c + \frac{Q}{n} dt c_0 \delta\left(x - x_c\right)\delta\left(t - t'_c\right), \tag{A45}$$

665 where δ is the Dirac delta (impulse) function, x_c is the location of the instantaneous point source, t'_c is the time at which the instantaneous point source is activated, Q is the fluid injection rate, and n is the aquifer porosity.

Analytical solution

The analytical solution of Eq. A45 has been derived by Bear (1979) considering the following conditions.

1. Boundary conditions (Neumann or second type):

670     $c, \nabla c = 0, \quad x = \pm\infty$.

2. Initial conditions:

    $c(x, t = 0) = 0, \quad -\infty < x < \infty$ at $t = 0$.

The solution reads as follows:

$$c(x) = \frac{c_0 Q}{4n\pi\gamma D_x} \exp\left[\frac{\nu(x-x_0)}{2D_x}\right] \frac{1}{t} \exp\left[-\left(\frac{\nu^2}{4D_x}\right)\tau - \frac{(x-x_c)^2}{4D_x\tau}\right], \tag{A46}$$

675 and can be used for solutes that are non-reactive (Test 7) or reactive (Test 8) by setting $\lambda = 0$ in Test 7. The derivation was
performed assuming (1) fluid with constant density and viscosity, (2) solute subject to first-order chemical transformation, (3)
constant and uniform flow and velocity in the x-direction, and (4) constant longitudinal dispersion coefficient (D). The solution
has a mathematical singularity in the point source region (Abdelaziz et al., 2013) because it takes the form of the exponential
integral when both $x - x_c$ approaches zero, hence becoming infinite at $\tau = 0$. However, according to Wexler (1989) the solution
680 is still valid as long as $(x - x_c)^2$ is larger than ν^2, as it is the case in our simulation tests.

A7 Tests 9 and 10 - Reactive and non-reactive transport with continuous point source

Governing equations

Similarly to the previous case, Tests 9 and 10 have only been performed for SUMMA-OpenWQ due to the same reasons. The
governing equation presented above in Eq. A44 is used here, but the derivation of the analytical condition is performed using
685 different initial conditions and boundary conditions, as detailed below.

Analytical solution

Wexler (1992) proposes to derive the governing Eq. A44 for a continuous point source using the following conditions:

1. Boundary conditions (Dirichlet or first type):

$$c, \nabla c = c_0 \quad x = 0,$$
690 $$c, \frac{dc}{dx} = 0 \quad x = \pm\infty\,.$$

2. Initial conditions:

$$c(x, t = 0) = 0, \quad -\infty < x < \infty \text{ at } t = 0\,.$$

The derivation was performed after modification from Bear (1979) and Genuchten and Alves (1982), and it reads

$$c(x) = \frac{c_0}{2}\left\{\exp\left[\frac{x}{2D_x}(\nu - U)\right]\text{erfc}\left[\frac{x - Ut}{2\sqrt{D_x t}}\right]\right.$$
695 $$\left. + \exp\left[\frac{x}{2D_x}(\nu + U)\right]\text{erfc}\left[\frac{x + Ut}{2\sqrt{D_x t}}\right]\right\}, \tag{A47}$$

where c_0 is the concentration of the continuous point source, $U = \sqrt{\nu^2 + 4\lambda D}$ and erfc is the complementary error function.
Parameter λ is the first-order reaction rate used for Test 10, which can be set to zero for Test 9.

Author contributions. Diogo Costa (Conceptualization, Data Curation, Formal Analysis, Funding Acquisition, Investigation, Methodology, Resources, Software, Supervision, Validation, Visualization, Writing – Original Draft Preparation, Writing – Review & Editing); Kyle Klenk
700 (Resources, Software, Writing – Review & Editing); Wouter Knoben (Writing – Review & Editing); Andrew Ireson (Writing – Review & Editing); Raymond J. Spiteri (Formal Analysis, Funding Acquisition, Methodology, Resources, Software, Supervision, Writing – Review & Editing.); Martyn Clark (Conceptualization, Formal Analysis, Funding Acquisition, Methodology, Resources, Software, Supervision, Writing – Review & Editing)

Competing interests. The authors declare that they have no conflict of interest.

705

Acknowledgements. This work was supported by the NSERC-Alliance Grant ALLRP 571910-22. We acknowledge support from Environment and Climate Change Canada, the Global Water Futures programme, and the Natural Sciences and Engineering Research Council of Canada under Discovery Grant RGPN-2020-04467 (RJS).

References

710 Hydrological Simulation Program–Fortran, User's manual for version 11: U.S. Environmental Protection Agency, National Exposure Research Laboratory, Athens, Ga., EPA/600/R-97/080, 755 p, 1997.

A semi-distributed ntegrated itrogen model for multiple source assessment in tchments (INCA): Part I — model structure and process equations, Science of The Total Environment, 210-211, 547–558, https://doi.org/10.1016/S0048-9697(98)00037-0, 1998.

Abdelaziz, R., Pearson, A., and Merkel, B.: Lattice Boltzmann modeling for tracer test analysis in a fractured Gneiss aquifer, Natural Science, 715   5, 368–374, https://doi.org/10.4236/ns.2013.53050, 2013.

Arnold, J. G., Moriasi, D. N., Gassman, P. W., Abbaspour, K. C., White, M. J., Srinivasan, R., Santhi, C., Harmel, R. D., Griensven, a. V., VanLiew, M. W., Kannan, N., and Jha, M. K.: SWAT: Model Use, Calibration, and Validation, Trans. ASABE, 55, 1491–1508, 2012.

Bear, J.: Hydraulics of groundwater, McGraw-Hill series in water resources and environmental engineering. McGraw-Hill, New York, 1979.

Beck, M. B.: Water quality modeling: A review of the analysis of uncertainty, Water Resources Research, 23, 1393–1442, 720   https://doi.org/10.1029/WR023i008p01393, 1987.

Bedekar, V., Morway, E. D., Langevin, C. D., and Tonkin, M. J.: MT3D-USGS version 1: A U.S. Geological Survey release of MT3DMS updated with new and expanded transport capabilities for use with MODFLOW, Tech. rep., Reston, VA, https://doi.org/10.3133/tm6A53, 2016.

Bosch, D., Theurer, F., Bingner, R., and Felton, G.: Evaluation of the AnnAGNPS water quality model, Agricultural Non-Point Source Water 725   Quality Models: Their Use and Application; John, EP, Daniel, LT, Rodney, LH, Eds, pp. 45–54, 1998.

Brown, L. and Barnwell, T.: The enhanced stream water quality models QUAL2E and QUAL2E-UNCAS: documentation and user manual, Environmental Protection Agency, 1987.

Celia, M. A., Bouloutas, E. T., and Zarba, R. L.: A general mass-conservative numerical solution for the unsaturated flow equation, Water Resources Research, 26, 1483–1496, https://doi.org/https://doi.org/10.1029/WR026i007p01483, 1990.

730 Clark, M. P. and Kavetski, D.: Ancient numerical daemons of conceptual hydrological modeling: 1. Fidelity and efficiency of time stepping schemes, Water Resources Research, 46, https://doi.org/https://doi.org/10.1029/2009WR008894, 2010.

Clark, M. P., Kavetski, D., and Fenicia, F.: Pursuing the method of multiple working hypotheses for hydrological modeling, Water Resources Research, 47, https://doi.org/https://doi.org/10.1029/2010WR009827, 2011.

Clark, M. P., Nijssen, B., Lundquist, J. D., Kavetski, D., Rupp, D. E., Woods, R. A., Freer, J. E., Gutmann, E. D., Wood, A. W., Brekke, L. D., 735   Arnold, J. R., Gochis, D. J., and Rasmussen, R. M.: A unified approach for process-based hydrologic modeling: 1. Modeling concept, Water Resources Research, 51, 2498–2514, https://doi.org/https://doi.org/10.1002/2015WR017198, 2015a.

Clark, M. P., Nijssen, B., Lundquist, J. D., Kavetski, D., Rupp, D. E., Woods, R. A., Freer, J. E., Gutmann, E. D., Wood, A. W., Gochis, D. J., Rasmussen, R. M., Tarboton, D. G., Mahat, V., Flerchinger, G. N., and Marks, D. G.: A unified approach for process-based hydrologic modeling: 2. Model implementation and case studies, Water Resources Research, 51, 2515–2542, 740   https://doi.org/https://doi.org/10.1002/2015WR017200, 2015b.

Clark, M. P., Zolfaghari, R., Green, K. R., Trim, S., Knoben, W. J. M., Bennett, A., Nijssen, B., Ireson, A., and Spiteri, R. J.: The Numerical Implementation of Land Models: Problem Formulation and Laugh Tests, Journal of Hydrometeorology, 22, 1627 – 1648, https://doi.org/10.1175/JHM-D-20-0175.1, 2021a.

Clark, M. P., Zolfaghari, R., Green, K. R., Trim, S., Knoben, W. J. M., Bennett, A., Nijssen, B., Ireson, A., and Spiteri, R. J.: The
745   Numerical Implementation of Land Models: Problem Formulation and Laugh Tests, Journal of Hydrometeorology, 22, 1627 – 1648,
       https://doi.org/https://doi.org/10.1175/JHM-D-20-0175.1, 2021b.

Costa, D. and Pomeroy, J. W.: Preferential meltwater flowpaths as a driver of preferential elution of chemicals from melting snowpacks,
       Science of The Total Environment, 662, 110–120, https://doi.org/10.1016/J.SCITOTENV.2019.01.091, 2019.

Costa, D., Burlando, P., and Liong, S.-Y.: Coupling spatially distributed river and groundwater transport models
750   to investigate contaminant dynamics at river corridor scales, Environmental Modelling & Software, 86, 91–110,
       https://doi.org/https://doi.org/10.1016/j.envsoft.2016.09.009, 2016.

Costa, D., Liu, J., Roste, J., and Elliott, J.: Temporal Dynamics of Snowmelt Nutrient Release from Snow–Plant Residue
       Mixtures: An Experimental Analysis and Mathematical Model Development, Journal of Environmental Quality, 48, 869–879,
       https://doi.org/https://doi.org/10.2134/jeq2018.12.0440, 2019.

755 Costa, D., Baulch, H., Elliott, J., Pomeroy, J., and Wheater, H.: Modelling nutrient dynamics in cold agricultural catchments: A review,
       Environmental Modelling & Software, 124, 104 586, https://doi.org/https://doi.org/10.1016/j.envsoft.2019.104586, 2020a.

Costa, D., Baulch, H., Elliott, J., Pomeroy, J., and Wheater, H.: Modelling nutrient dynamics in cold agricultural catchments: A review,
       Environmental Modelling & Software, 124, 104 586, https://doi.org/https://doi.org/10.1016/j.envsoft.2019.104586, 2020b.

Costa, D., Shook, K., Spence, C., Elliott, J., Baulch, H., Wilson, H., and Pomeroy, J. W.: Predicting Variable Contributing Areas, Hydro-
760   logical Connectivity, and Solute Transport Pathways for a Canadian Prairie Basin, Water Resources Research, 56, e2020WR027 984,
       https://doi.org/https://doi.org/10.1029/2020WR027984, 2020c.

Costa, D., Pomeroy, J. W., Brown, T., Baulch, H., Elliott, J., and Macrae, M.: Advances in the simulation of nutrient dynamics in cold climate
       agricultural basins: Developing new nitrogen and phosphorus modules for the Cold Regions Hydrological Modelling Platform, Journal of
       Hydrology, 603, 126 901, https://doi.org/https://doi.org/10.1016/j.jhydrol.2021.126901, 2021.

765 Costa, D., Sutter, C., Shepherd, A., Jarvie, H., Wilson, H., Elliott, J., Liu, J., and Macrae, M.: Impact of climate change on catchment nutrient
       dynamics: insights from around the world, Environmental Reviews, 0, null, https://doi.org/10.1139/er-2021-0109, 2022.

Davies, T. D., Brimblecombe, P., Tranter, M., Tsiouris, S., Vincent, C. E., Abrahams, P., and Blackwood, I. L.: The Removal of Soluble Ions
       from Melting Snowpacks, Springer Netherlands, Dordrecht, https://doi.org/10.1007/978-94-009-3947-9_20, 1987.

Di Toro, D. M., Fitzpatrick, J. J., Thomann, R. V., and Hydroscience, I.: Documentation For Water Quality Analysis Simulation Program
770   (WASP) And Model Verification Program (MVP), Tech. rep., 1983.

Genuchten, M. T. and Alves, W.: Analytical solutions of the one-dimensional convective-dispersive solute transport equation, US Department
       of Agriculture, 1982.

Harbaugh, A. W.: MODFLOW-2005, the US Geological Survey modular ground-water model: the ground-water flow process, vol. 6, US
       Department of the Interior, US Geological Survey Reston, VA, USA, 2005.

775 Hutton, E. W., Piper, M. D., and Tucker, G. E.: The Basic Model Interface 2.0: A standard interface for coupling numerical models in the
       geosciences, Journal of Open Source Software, 5, 2317, https://doi.org/10.21105/joss.02317, 2020.

Jackson-Blake, L. A., Wade, A. J., Futter, M. N., Butterfield, D., Couture, R.-M., Cox, B. A., Crossman, J., Ekholm, P., Halliday, S. J., Jin, L.,
       Lawrence, D. S. L., Lepistö, A., Lin, Y., Rankinen, K., and Whitehead, P. G.: The INtegrated CAtchment model of phosphorus dynamics
       (INCA-P): Description and demonstration of new model structure and equations, Environmental Modelling & Software, 83, 356–386,
780   https://doi.org/10.1016/J.ENVSOFT.2016.05.022, 2016.

Jones, H. G.: The ecology of snow-covered systems: a brief overview of nutrient cycling and life in the cold, Hydrological Processes, 13, 2135–2147, https://doi.org/10.1002/(SICI)1099-1085(199910)13:14/15<2135::AID-HYP862>3.0.CO;2-Y, 1999.

Lesser, G., Roelvink, J., van Kester, J., and Stelling, G.: Development and validation of a three-dimensional morphological model, Coastal Engineering, 51, 883–915, https://doi.org/https://doi.org/10.1016/j.coastaleng.2004.07.014, coastal Morphodynamic Modeling, 2004.

785 Lilbaek, G. and Pomeroy, J. W.: Modelling enhanced infiltration of snowmelt ions into frozen soil, Hydrological Processes, 21, 2641–2649, https://doi.org/10.1002/hyp.6788, 2007.

Lindström, G., Pers, C., Rosberg, J., Strömqvist, J., and Arheimer, B.: Development and testing of the HYPE (Hydrological Predictions for the Environment) water quality model for different spatial scales, Hydrology Research, 41, 295, https://doi.org/10.2166/nh.2010.007, 2010.

790 Marsh, P. and Pomeroy, J. W.: Spatial and temporal variations in snowmelt runoff chemistry, Northwest Territories, Canada, Water Resources Research, 35, 1559–1567, https://doi.org/10.1029/1998WR900109, 1999.

Mekonnen, B. A.: Modeling and management of water quantity and quality in cold-climate Prairie Watersheds, Ph.D. thesis, University of Saskatchewan, 2016.

Moore, D. S., Bingner, R. L., and Theurer, F. D.: ANNAGNPS: Accounting for Snowpack, Snowmelt, and Soil Freeze-Thaw, in: Eighth
795 Federal Interagency Sedimentation Conference (8thFISC),, pp. 475–482, Reno, NV, USA, 2006.

Partow, A.: ExprTk C++ Mathematical Expression Library, https://www.partow.net/programming/exprtk/, 1999.

Peckham, S. D., Hutton, E. W., and Norris, B.: A component-based approach to integrated modeling in the geosciences: The design of CSDMS, Computers & Geosciences, 53, 3–12, 2013.

Pomeroy, J., Davies, T., Jones, H., and Marsh, P.: Transformations of snow chemistry in the boreal forest: accumulation and volatilization,
800 Hydrological Processes, 13, 2257–2273, 1999.

Pomeroy, J., Brown, T., Fang, X., Shook, K., Pradhananga, D., Armstrong, R., Harder, P., Marsh, C., Costa, D., Krogh, S., Aubry-Wake, C., Annand, H., Lawford, P., He, Z., Kompanizare, M., and Lopez Moreno, J.: The cold regions hydrological modelling platform for hydrological diagnosis and prediction based on process understanding, Journal of Hydrology, 615, 128 711, https://doi.org/https://doi.org/10.1016/j.jhydrol.2022.128711, 2022.

805 Pomeroy, J. W., Davies, T. D., and Tranter, M.: The Impact of Blowing Snow on Snow Chemistry, in: Seasonal Snowpacks: Processes of Compositional Change, pp. 71–113, Springer, Berlin, Heidelberg, https://doi.org/10.1007/978-3-642-75112-7_4, 1991.

Pomeroy, J. W., Gray, D. M., Brown, T., Hedstrom, N. R., Quinton, W. L., Granger, R. J., and Carey, S. K.: The cold regions hydrological model: A platform for basing process representation and model structure on physical evidence, Hydrological Processes, 21, 2650–2667, https://doi.org/10.1002/hyp.6787, 2007.

810 Refsgaard, J. and Storm, B.: MIKE SHE.[in:] Singh VP (ed.), Computer Models of Watershed Hydrology, Water Resources Publication, Colorado, pp. 809–847, 1995.

Richmond, B.: An introduction to systems thinking with STELLA, ISEE systems, ISBN-10: 0970492111, 2004.

Saloranta, T. M. and Andersen, T.: MyLake—A multi-year lake simulation model code suitable for uncertainty and sensitivity analysis simulations, Ecological Modelling, 207, 45–60, https://doi.org/https://doi.org/10.1016/j.ecolmodel.2007.03.018, uncertainty in Ecological
815 Models, 2007.

Sanderson, C. and Curtin, R.: Armadillo: a template-based C++ library for linear algebra, Journal of Open Source Software, 1, 26, https://doi.org/10.21105/joss.00026, 2016.

Sanderson, C. and Curtin, R.: A User-Friendly Hybrid Sparse Matrix Class in C++, pp. 422–430, https://doi.org/10.1007/978-3-319-96418-8_50, 2018.

820   Shoemaker, L.: Compendium of tools for watershed assessment and TMDL development, https://nepis.epa.gov/Exe/ZyPURL.cgi?Dockey=20004NX4.TXT, 1997.

Streeter, H. and Phelps, E.: A Study of the Pollution and Natural Purification of the Ohio River. III. Factors Concerned in the Phenomena of Oxidation and Reaeration, U.S. Government Printing Office, 1925.

Trefry, M. G. and Muffels, C.: FEFLOW: A Finite-Element Ground Water Flow and Transport Modeling Tool, Groundwater, 45, 525–528,
825   https://doi.org/https://doi.org/10.1111/j.1745-6584.2007.00358.x, 2007.

Wade, A., Jackson, B., and Butterfield, D.: Over-parameterised, uncertain 'mathematical marionettes' — How can we best use catchment water quality models? An example of an 80-year catchment-scale nutrient balance, Science of The Total Environment, 400, 52–74, https://doi.org/10.1016/j.scitotenv.2008.04.030, 2008.

Wade, A. J., Durand, P., Beaujouan, V., Wessel, W. W., Raat, K. J., Whitehead, P. G., Butterfield, D., Rankinen, K., and Lepisto, A.: A
830   nitrogen model for European catchments: INCA, new model structure and equations, Hydrology and Earth System Sciences, 6, 559–582, https://doi.org/10.5194/hess-6-559-2002, 2002.

Wexler, E. J.: Analytical solutions for one-, two-, and three-dimensional solute transport in ground-water systems with uniform flow, Tech. rep., https://doi.org/10.3133/ofr8956, 1989.

Wexler, E. J.: Analytical solutions for one-, two-, and three-dimensional solute transport in ground-water systems with uniform flow, US
835   Government Printing Office, 1992.

Whitehead, P., Wilson, E., Butterfield, D., and Seed, K.: A semi-distributed integrated flow and nitrogen model for multiple source assessment in catchments (INCA): Part II — application to large river basins in south Wales and eastern England, Science of The Total Environment, 210-211, 559–583, https://doi.org/https://doi.org/10.1016/S0048-9697(98)00038-2, 1998.

Woldegiorgis, B. T., Baulch, H., Wheater, H., Crossman, J., Clark, M., Stadnyk, T., and Bajracharya, A.: Impacts of uncontrolled operator
840   splitting methods on parameter identification, prediction uncertainty, and subsurface flux representation in conceptual hydrological models, Water Resources Research, 59, e2022WR033 250, 2023.

Wool, T., Ambrose, R. B., Martin, J. L., and Comer, A.: WASP 8: The Next Generation in the 50-year Evolution of USEPA's Water Quality Model, Water, 12, https://doi.org/10.3390/w12051398, 2020.

Yang, X., Tetzlaff, D., Soulsby, C., and Borchardt, D.: HiWaQ v1.0: A flexible catchment water quality assessment tool with compatibility for
845   multiple hydrological model structures, Geoscientific Model Development Discussions, 2022, 1–26, https://doi.org/10.5194/gmd-2022-239, 2022.